

Some inductive properties of nanocomposites : water.*)

Gheorghe Dragan ,
GDF – DATA BANKS , Str Abrud 25 , Bucharest 78186, ROMANIA
(gdf@fx.ro)

Introduction

Composite structure of liquids was recently reviewed and revealed by analyzing representative data on vapor-liquid equilibria* by considering topoenergetic principles in retrieval of experimental data and to establish their structural significances [1]. Even so-called pure liquids represented by unique molecular species results to be multiphase systems. Water is a particular case for which many experimental data can prove this fact. Generally, two main phases are detected in different conditions of behaviour, namely the amorphous phase responsible for instance for mixing with gases, solid solutes and/or other liquids while the “crystalline” one remains as inert. These two phases are intimately mixed each other with dimensions of nm as order of magnitude and the macroscopic properties of liquids depend on the nature and strength of their coupling. This aspect represents the main purpose of the present contribution regarding water and aqueous solutions.

Topoenergetic point of view

The composite structure of systems under transformation was the basic principle in the development of new working principles in defining the behaviour of any kind of system in different processing and/or operating conditions. The physical meaning of this assumption is that in a transforming system at least two components (phases) coexist, mutually interact and exchange energy with exterior in different manners. In view to better understand the evolution of these new working principles, the main milestones of their development are presented below.

The experimental study of polymer morphology, more exact of polyethylenes, represented the starting point of the development of these new principles. Polyethylene (PE) is a so-called semicrystalline polymer having amorphous and crystalline phases. In ideal conditions PE has a planar zigzag catena (Annex 1) which defines the molecular conformation (molecular geometry), but in different synthesis conditions two important PE types result, namely : low density (LDPE) and high density (HDPE) in which the nature and density of molecular defects are different. Generally, the crystalline morphology common for both PE types has lamellar habit with orthorhombic unit cell [2], but its behaviour in different processing and/or operating conditions drastically differs.

Annealing at temperatures near melting point of crystalline phase is one of the important treatment applied to polymer samples in view to stabilize their

* Paper presented at Nanotubes and Nanostructures 2001, INF Frascati, Rome, 17-27 Oct 2001

morphology. Two independent processes occur in crystalline phase, namely the lamellar thickening and precipitation of intralamellar defects (Annex 2). The ratio of amplitude associated to these processes is different for the two kinds of PE, namely: in HDPE predominates lamellar thickening while in LDPE predominates the defect precipitation. This last process has an important effect on the behaviour of crystalline phase and has been initially detected by multimelting behaviour in a highly branched PE (LDPE) subsequently annealed at increasing temperatures in steps of 5^oC below melting point [4]. The nature of this process was thoroughly studied on some HDPE brands and the samples obtained by their chlorination (CPE) [5-7]. Conformational defects randomly distributed in crystalline phase of HDPE were grafted by chlorination in aqueous suspension and activated by UV radiation, so CPE samples behave in annealing treatment like LDPE. In fact, the intralamellar defects coherently precipitate into local amorphous domains (LAD) along the direction defined by minimum elastic constant [8]. Melting behaviour of these samples gives interesting information about the **nature and amplitude** of this process. It is important to reveal these two main aspects unequivocally defining the transformation process. Melting process can be evidenced by the dependence of specific heat (at constant pressure, Cp) as a function of temperature. There are many calorimetric measuring systems allowing such measurements. Adiabatic calorimeters with small heat increments are the most accurate, but need long time and laborious experimental conditions. Differential thermal analyzers (DTA) and differential scanning calorimeters (DSC) are enough accurate for rapid analysis and comparison of large series of related samples. In calorimetric systems melting of the crystalline phase produced by increasing temperature appears as an increasing dependence of Cp(T) having a lambda shape extended over a specific temperature range and centered on the maximum value of Cp defining melting point denoted as T_{m0}. This Cp(T) dependence is specific to an order-disorder process [9]. DTA melting behaviour of HDPE and its CPE annealed at a temperature near T_{m0} for different periods of time, show that by annealing the melting endotherm of HDPE becomes sharper, taller and T_{m0} shifts to higher values, while for CPE it appears a lower endotherm centered on T_{m1} temperature, increasing in amplitude with annealing time while T_{m0} proportionally decreases. Conversion of splitting coefficient (α) during annealing at different temperatures shows that there is a threshold temperature below which this splitting process does not exist. This value represents the glass transition (T_g \approx 80 ^oC) for molecular species of polyvinylchloride obtained in CPE samples.

T_{m1} melting process represents also an order to disorder process and is associated to the "melting" of ordered LAD. T_{m1} and T_{m0} processes appear to be strongly interconnected evidencing the coupling of the two phases: LAD and crystalline fragments. A similar coupling may exist also in HDPE between crystalline and amorphous phases and can be generalized to any crystalline material influencing its melting, crystallization and all properties. This coupling appears in DTA measuring system by melting endotherms, so it is important to analyze how these processes can be described.

Oster & Auslander assumed that a transforming system can be described as electric circuits by contribution of components with elementary behaviour

(dissipative, capacitive, inductive, potentials, etc.), called as **topoenergetic representation of non-equilibrium systems** [10]. Unfortunately, they tried to describe just at beginning complicated cases by considering spatial distribution of energy circuits and could not verify experimental results, so they abandoned soon these ideas. The above results have allowed to represent the overall ATD measuring system as an energy circuit in which the tested specimen consists in two capacitive components dissipatively coupled (Annex 3) [11]. It is important to note that space does not appear explicitly, but is implicitly contained in the constitutive components. For instance, if one compares the results for the same sample obtained in different DTA systems having different shapes and dimensions, they differ, so it is of capital importance to standardize the shape and dimensions of the tested specimens and generally the experimental conditions in view to compare the behaviour of different samples.

The time dependence of energy flow for each capacitive component appears as essential aspect of this new formalism, so the two coupling components of the tested specimen have their own local time frames. The inert component, C_{in} , has the same time frame as the inert component of the reference specimen (CR), but the local time frame of the transforming component, C_{tr} , is different. Experimentally, this fact shows that the associated heat flow w_{in} immediately appears by changing exterior temperature T_1 , while w_{tr} is delayed as a function of temperature and process nature.

The study of the amorphous-crystalline coupling in HDPE has the first application of these basic concepts for which the approximation of purely dissipative coupling was assumed (Annex 4)[12]. T_{mo} represents the threshold value which separates the two processes: crystallization ($T < T_{mo}$) and melting ($T > T_{mo}$). Crystallization process was initially considered by using an isothermal differential calorimeter prepared at a crystallization temperature, T , where the tested specimen was transferred from an initial equilibrium temperature over T_{mo} . Two exothermal heat flows appear, namely the first one immediately after the contact of the specimen with the calorimeter cell is w_{in} and the delayed one, w_{tr} . (see Annex 5: superimposed crystallization thermograms obtained for a polyester brand on standard specimens at crystallization temperatures spaced at 1°C in a commercial DSC). The period t_i depends on T according to a kinetic eqn. established by considering the Arrhenius law for specific period of time associated to local thermal transfer of C_{tr} . For a series of similar experiments performed in standardized experimental conditions (SEC) for different crystallization temperatures, it is possible to determine the constant (E , K) defining the nature and amplitude of crystallization process. Annex 6 shows the experimental results according to the original Arrhenius kinetic eqn. obtained in SEC for three HDPE brands. There are represented two series of data obtained for dry samples (powder as such) and their mixture with silicon oil (medium samples) considered as inert component.

This kinetic eqn. and all experimental procedure were extended soon to a large variety of transforming processes. Annex 7 presents the results obtained for the curing-polymerization process in a mixture of epoxide resin/curing agent for which the threshold temperature is the glass transition of the epoxide resin or a specific value of the mixture defining its freezing point [13].

By considering a large number and variety of transforming processes according to the specific SEC and a general procedure, a UNIVERSAL representation was established (Annex 8) [7,14].

Annex 9 presents the results for crystallization process of HDPE samples according to these principles. In both representations the process nature is common for all tested samples and defined by first phylogenic parameters (n1,m1) while the amplitude can be defined by ontogenic parameters. For instance, the amplitude of crystallization process is defined by the content in crystalline phase initially determined by DTA [15], so it results a good agreement with the value predicted by K parameter (see its significance in the Annex 4).

Annex 10 sketches again the main features of the topoenergetic principles in defining the behaviour of composite systems in Arrhenius and Universal representations. Polarity of the transforming process is another important aspect defining the particular significance of the ontogenic and phylogenic parameters. For instance, the crystallization and polymerization processes have different polarities as it results immediately by comparing their calorimetric thermograms [16]. Relationships presented in the table are established by analyzing a large variety of practical cases, but CS (the coupling strength of Cin and Ctr) these are not definite yet.

The model of purely dissipative coupling has been tried also for the coupling of LAD-crystalline fragments in CPE sample in annealing experiments similar to the crystallization ones (Annex 11) [17]. This coupling was initially studied by considering the time conversion of the splitting coefficient as determined by DTA on already annealed CPE samples (considered as *in vitro* measuring system), so *live* experiments (*in vivo* measuring system) systematically showed only the inert component and never the transforming process, but the DTA on the resulted samples clearly showed the defect precipitation and LAD formation. It appears that an inductive component appears in this particular amorphous-crystalline coupling, CL, whose energy flow annihilates: $w_{tr} = -w_L$. This can be explained by the direction change of the kinetic momentum of precipitating defects. These experimental facts are similar with the apparently violation of conservation laws for energy and kinetic momentum evidenced in β -decay process also by calorimetry [18,19]. These facts were led to the consideration of neutrino as a new particle whose existence is not yet clearly confirmed by experiments.

The next step was to check if an inductive effect exists by simultaneous annealing of two identical CPE [20] or different samples [21]. Annex 12 shows details of these experiments performed by using a brass block for isothermally annealing of CPE medium samples. The annealed samples have cylindrical shape with diameter of 6 mm and were cut at the same height as DTA specimens in view to perform 4-6 DTA runs on each sample and to determine the mean and standard deviation values for the splitting coefficient. Annex 13 shows the obtained results as a function of annealing time for the same CPE medium sample as annealed in different orientation in respect to gravitational field and/or each to other, namely only vertical (V) or only horizontal (H), simultaneously annealed vertical and horizontal (VH) and simultaneously annealed two vertical samples (VV). Two series of results are obtained by placing the samples directly in metallic block and in Pyrex glass tubes,

respectively. A clear difference results for the first series of results, so the early stage of defect precipitation expressed by the splitting coefficient at 1 minute of annealing (α_0) shows a net inductive interaction both with the gravitational field and between them depending on the mutual orientation (Annex 12).

Water and aqueous solutions

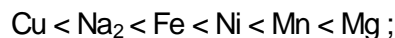
The initial idea on composite structure of liquids was based on the observations of solubility behaviour. These observations belong to the general observations according to which not entire specimen participates to any kind of transforming process. In solubility experiments the process of transformation is triggered by isothermally mixing of two components (Annex 14). Once again calorimetry is the most appropriate measuring system for such processes. High resolution mixing calorimetry (HRMC) allows to reveal many important aspects of these processes in most efficient conditions [22]. Solution and dilution processes of several sulfates (as anhydrous and hydrated species) in water have revealed the composite structure of water and aqueous solutions, the nature and amplitude of these processes. The net difference between structure of water used as solvent and water contained in the hydrated species was the first important fact observed. Hydrated species show endothermal solution process while anhydrous ones have exothermal effect. It results that cations create specific ordered domains in aqueous solutions.

Annex 15 shows the first phylogeny in Arrhenius representation of solubility behaviour of several hydrated species of alkali halides salts in water as expressed in grams of anhydrous salt per gram of water (eigenvalue) [23]. Even for an experimented scientist, it would be no difference between solubility behaviour of different hydrated and anhydrous species of the same salt. Although their nature seems to be the same in this representation, the amplitude strongly differs for the same salt, showing that the solution process involves only a specific phase of water considered as amorphous.

Annex 16 presents the dependences of h_s and E_s of solution endotherms for two fractions of $\text{NiSO}_4 \cdot 7\text{H}_2\text{O}$ grain size as a function of solute mass (m_{st}) at room temperature [22,24]. It results a common phylogeny for water solubility of all considered sulfates by considering $\theta = h_s$ or E_s and $U = m_{st}$ ($U_0 = 0$).

Annex 17 shows the dependences of h_d of HRMC dilution thermograms as a function of c_{st} (concentration of diluted solutions in mass of anhydrous sulfate per mass of water) at room temperature.

Annex 18 shows the dependences of most important topoenergetic parameters in Universal representation of dilution processes of the considered sulfates for $\theta = E_d$ and $U = c_{st}$ ($U_0 = 0$) (at 30°C) [22]. The significance of these results is similar to the results obtained for solution processes, namely: the nature is the same; the amplitude of solution process increases in the following order with the cation species :



the kinetic entity and the coupling strength (CS) between the newly formed amorphous phase in the aqueous solutions and the "crystalline" phase (as the

inert component in dilution and solution processes) have inverse order in the series. CS dependence is supported by further measurements.

Hosemann and coworkers have demonstrated for a large variety of materials (metals and polymers) by using an original and accurate small angle X-ray scattering technique, that amorphous and crystalline phases remain as separated and have similar structures in molten and solid states [25].

The next step in the structural study of water and aqueous solutions is to reveal more direct the existence of the amorphous-crystalline coupling similar to the one observed in PE.

Annex 19 shows in its upper part the DSC measuring system used for evidence of melting behaviour of water and aqueous solutions [24]. A standardized specimen and thermal regime of freezing and heating were used. The melting endotherms of a series of successively diluted to half concentration of aqueous solutions of $\text{CuSO}_4 \cdot 5\text{H}_2\text{O}$ and water (solvent) are represented in the lower part. For all considered sulfates the same splitting phenomenon like for CPE was observed, proportional with cst.

Annex 20 shows the dependences of some important parameters measured on melting endotherms as a function of cst for several sulfates. In addition (see Annex 2 for CPE) it was considered: the overall melting enthalpy for pure water and for a solution ($\Delta H_m(\text{cst})$); their ratio, $q = 100(\Delta H_m(\text{cst}) / \Delta H_m(0))$, (in %), representing the percentage modification of the melting of water by solute addition; αq and $(1-\alpha)q$ the similar modification associated to T_{m1} and T_{m0} processes, respectively. Dependences of h_1 and α on cst are similar to the stress-strain dependences, so they are comparable taking into account the common process of defect and/or impurity precipitation activated by thermal and mechanical energy, respectively. Na_2 has the most "rigid" behaviour, while Mn shows a plastic flow of precipitates, corresponding to strong and weak binding of precipitates, respectively. The same significance results for the dependences of αq and $(1-\alpha)q$ on cst. These facts are in good agreement with the result for the coupling strength between C_{in} and C_{tr} in dilution behaviour (Annex 18).

It results that thermomechanic analysis (TMA) of melting process could evidence this amorphous-crystalline coupling in more accurate conditions than DSC. Annex 21 shows schematic draw of the basic disposition for accurate measurements of density of liquid samples, differential thermal density analysis (DTDA) and TMA [24]. Annex 22 schematically shows details of TMA principle.

Annex 23 shows typical melting thermograms and the significances of some important quantities measured from DTDA and TMA runs for aqueous solutions. The most important fact is that by freezing of aqueous specimens in highly repeatable conditions, the thermally driven separation process between amorphous and crystalline phases can observe by telescopic shearing (see detail in Annex 22). The same process was observed in DSC cell for which splitting process occurred.

Annex 24 reproduces DTDA and TMA thermograms for a series of aqueous solutions obtained by successively dilution to half concentration in comparison with pure water used as the solvent.

Annex 25 shows the dependence of $E_1(E_0)$ (both quantities expressed in arbitrary units from recorded diagrams) as resulted from TMA for different

aqueous solutions of the considered sulfates. The same significance results for the cation influence as from DSC.

Annex 26 shows the dependence of internal stresses between frozen and liquid states, σ_{int} , and percentage modification of liquid density by solute addition versus c_{st} for several considered solution series. It is important to note: (i) solute addition decreases internal stresses and (ii) the effect of Mn is higher than Na₂, i.e. at the same c_{st} : $\sigma_{int}(Na_2) > \sigma_{int}(Mn)$ in good agreement with the coupling strength in the liquid state. Liquid density shows that Na₂ makes more dense clusters than other cations make. A similar phenomenon has been evidenced for water in liquid state for which the internal stresses (as expressed independently by CS and threshold pressure) decrease by ethanol addition at 25°C [26].

Homoeopathy

Intensive and long experience on structure and properties of water and aqueous solution by using more and more sensitive experimental techniques, has allowed evidence the difficulties in obtaining reproducible samples even originating from the same sample of water. However, in view to evidence the influence of a specific treatment, these techniques have demonstrated their efficiency. For instance HRMC is enough sensitive, repeatable and/or reproducible measuring system in evidencing the endothermal effect of mixing of two specimens originating from the same water sample one of them held in the hand of the operator just before. The mixing effect without this “radiestezic treatment” was systematically zero even on 10 times higher sensitivity.

The coexistence of amorphous and crystalline phases in water and aqueous solutions is evidenced by HRMC experiments of the tested specimen with a hygroscopic liquid denoted as **structural developer** (ethanol, methanol, pyridine, amines, phenol, etc.) (Annex 27). The mixing exotherm shows a bimodal process, so the first one represents the mixing of the amorphous phase and the delayed one is specific to a part of the crystalline phase. For pure water or diluted solutions it is difficult to separate the two components in the thermogram. However, it is possible to consider the discrete form of the global exotherm, $w(t)$, at the same intervals of time for a series of repeated experiments in rigorously standardized experimental conditions.

Annex 28 shows the theoretical dependence of the integral mixing energy, $E(t)$ and relative standard deviation, $\sigma(t)$, on mixing time for a unimodal process [27].

Annex 29 shows experimental results of $\sigma(t)$ obtained at 30°C by using methanol as developer for different specimens of water and successively diluted aqueous solutions [27]. It is important to mention the following aspects on sample conditioning: H₂O STD is freshly distilled water which is essentially degassed; H₂O STD* is “dynamized” (or succussed) H₂O STD (a mechanical treatment specific to the homoeopathic technique consisting in vigorous beating the glass container with the liquid sample on a solid support (metallic bloc covered with a cotton tissue) for 100 times with an approximate frequency of 1 beat/second); annealed H₂O STD was freshly distilled water maintained at room temperature for approximately 3 months; normal solutions are obtained by simply addition of water (H₂O STD) on successively diluted solutions without

any agitation; succused solutions were performed by using annealed H₂O STD. There are evident differences for the three types of water samples, so that the annealing and succussion have the effect of equilibrating the composite structure of water by decreasing σ value in the following sequence:

H₂O STD > H₂O STD* > annealed H₂O STD.

Systematic differences in the normal and succused solutions result over approximately 50 seconds of mixing. In the first stage the weakest coupling structures are formed by chemical etching effect of the developer, so the minimum values mark the formation of stronger and stronger structures. H₂O STD clearly shows this separation and by addition of Na₃PO₄·12H₂O this separation increases, i.e. the first stage of weak coupling species is narrowed and the second stage increases.

Succused solutions show a broadening of the first stage due to the hardening process of the initial species.

Another important aspect corresponds to the oscillatory behaviour of σ as a function of dilution order for both series of solutions (left side of Annex 29). The amplitude of these oscillations is smaller for succused solutions, but the maxima are for the same orders: 1, 3, 5, 7.

Homoeopathy represents a so-called traditional medical practice using as remedies successively and dynamized aqueous solutions of initial tinctures generally described in *Materia Medica*. Homoeopathy is considered as founded by Samuel Hahnemann (see Annex 30) by experiencing the basic acting principle according to which an agent producing the disease can cure, but administered in specific low doses (“*similia similibus curantur*”).

Annex 31 schematically shows how homoeopathic (centesimal) dilutions are performed according to Hahnemann technique called as n-CH (n is the dilution order). It is important to note that the probability to find material traces of the initial tincture in dilutions over approximately n=6 is practically zero. However, homoeopathic practice usually prescribes CH dilutions up to n=200 and experiences systematic clinical effects. Could be these clinical effects similar or just placebo effect?

The first step in searching the answer was to detect stable and reproducible structural patterns in these dilutions. This idea was launched also for establishing efficient analytical methods in view to characterize the reproducibility of prescribed dilutions.

Natrium Murriaticum is one of the basic remedy prescribed by *Materia Medica* with CH dilutions made with 70% vol ethanol as the solvent. High accuracy measurements on liquid density by using above described technique (Annex 21) on normal and dynamized series of centesimal dilutions have showed systematic results appearing at first sight as contradictory by comparing with their ethanol content (Annex 31). The final conclusion demonstrated on further experiments was that ethanol makes more stable structures in dynamized dilutions.

Density and different calorimetric measurements on a large number of normal and dynamized centesimal dilutions have demonstrated systematic structural differences, but the results have large statistical deviations. For instance, the air

content cannot be controlled enough, and this is an important source of the majority of structural measurements.

The next step was to compare structural patterns with clinical results performed in most objective conditions. For this reason, the method of isolated organ was chosen as avoiding the placebo effect.

Annex 32 shows the classical experimental setup used for evidencing the contraction and/or relaxation effect of an acting agent on the isolated piece of duodenum smooth muscle taken from rat. Aqueous solution of acetylcholine was used as standard (contraction action) in respect to which the normal and dynamized centesimal dilutions (in pure water) of Belladonna was defined by pharmacodynamic activity (in %). Tincture of Belladonna is usually prescribed in general medical practice by its relaxation effect on duodenum muscle. Annex 33 presents pharmacodynamic action (PA) of centesimal dilutions of Belladonna as function of dilution order up to $n=200$ [28]. It is important to notice the following facts: pure water has no effect while dynamized water shows a reproducible and small contracting effect; normal dilutions show a vanishing relaxation effect up to $n=5$; PA of CH dilutions shows not monotonous dependence with n , furthermore over approximately $n=25$ it changes in contracting effect and becomes as oscillatory ; PA was repeated several times for each n (on different dilutions and piece of rat duodenum) and reproduces also after 18 months on the same dilutions (differences in both cases were up to 2%); CH dilutions up to approximately $n=40$ showed smell of ethanol for long time; highly accurate measurements on specific heat showed an approximately similar dependence as $PA(n)$, but with statistical deviations of repeated and reproduced experiments higher than PA values.

As a consequence of a large number of structural measurements on CH dilutions of different tinctures (using additionally other experimental techniques that the above mentioned ones) and correlated with clinical results, it is possible to assume the following

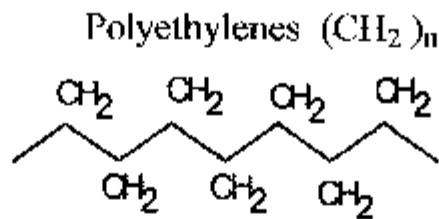
Conclusions :

1. Internal stresses in water and aqueous solutions are associated to amorphous-crystalline coupling. Generally, σ_{int} has maximum value in pure water and decreases with solute addition. They are responsible for macroscopic properties of aqueous samples both in liquid and solid state.
2. Structures of CH dilutions and $PA(n)$ information are established during performing CH dilutions. These must be considered as unitary, because the existence of the n -th dilution means that the entire series up to n already exists.
3. Efficient inductive components formed by succussion, together with other structural components in CH dilutions can transmit, receive and/or convert this information in different forms of energy specific to PA nature. It is possible as all dilutions have the same basic physical structure, but establishing a specific and permanent link with $PA(n)$. This linkage can be transferred to another support (for instance to sucrose granules).
4. $PA(n)$ as pure information not supported by classical forms of energy and/or mass becomes as resident in an **informational library**, so it is possible as this already contains this information before performing n -CH dilutions.

References

- [1] G.Dragan, *GDF Databanks Bulletin*, **2(1)**,3 (1998).
- [2] C.Nakafuku, *Polymer*, **19**, 149 (1978) ; *private communication*.
- [3] Y.Maeda & H.Kanetsuna, *J.Polymer Sci., Polymer Phys.Ed.*, **12**, 2551 (1974).
- [4] A.P.Gray & K.J.Casey, *J.Polym.Sci.*, **B 2**, 381 (1964).
- [5] G.Dragan, *J.Polym.Sci., Polymer Symposium*, **64**, 141 (1978).
- [6] G.Dragan, *Rev.Roumaine Chim.*, **26**, 1315 (1981).
- [7] G.Dragan, *Acta Polymerica*, **37**, 620 (1986).
- [8] T.Nagasawa & K.Kobayashi, *J.Appl.Phys.*, **41**, 4276 (1970).
- [9] M.E.Fisher, *The nature of critical points*, University of Colorado Press, 1965.
- [10] G.F.Oster & D.M.Auslander, *J.Franklin Institute*, **292**, 1;77 (1971).
- [11] G.Dragan, *J.Thermal Anal.*, **9**, 405 (1976); **15**, 297 (1979).
- [12] G.Dragan, *Rev.Roumaine Chim.*, **23**, 629 (1978).
- [13] G.Dragan & F.Stoenescu, *Rev.Roumaine Chim.*, **24**, 55 (1979).
- [14] G.Dragan, *Acta Polymerica*, **36**, 499 (1985).
- [15] G.Dragan, *Rev.Roumaine Chim.*, **20**, 687 (1975).
- [16] G.Dragan, *J.Thermal Anal.*, **23**, 173 (1982).
- [17] G.Dragan, *Rev.Roumaine Chim.*, **21**, 1381 (1976).
- [18] C.D.Ellis & W.A.Wooster, *Roy.Soc.Proc.*, **A 117**, 109 (1927).
- [19] L.Meitner & W.Orthmann, *Zeitschrift fur Physik*, **60**, 143 (1930).
- [20] G.Dragan, *Rev.Roumaine Chim.*, **21**, 1537 (1976).
- [21] G.Dragan, *Rev.Roumaine Chim.*, **23**, 1313 (1978).
- [22] G.Dragan, *J.Thermal Anal.*, **31**, 677; 941 (1986) ; **32**, 293 (1987).
- [23] M.Broul & J.Nyvt & O.Sohnel, "Solubility in inorganic two-component systems", Academy, Prague, 1981.
- [24] G.Dragan, *Acta Polymerica*, **38**, 211 (1987).
- [25] R.Hosemann & J.Loboda-Cackovic & H.Cackovic, *Ber.Bunsengesellschaft Phys.Chem.*, **77**, 1044 (1973).
- [26] G.Dragan, *GDF Databanks Bulletin*, **5**, 5 (2001).
- [27] G.Dragan, *J.Thermal Anal.*, **38**, 1497 (1992).
- [28] A.Cristea & G.Dragan, *Correlation of pharmacodynamic activity with some structural data of high aqueous dilutions of Belladonna*, Proceedings of the First national Conference on Homoeopathy, 12-13 October 1989, Sibiu (Romania).

(33 Annexes)



Molecular conformation (bond geometry) : planar zigzag catena

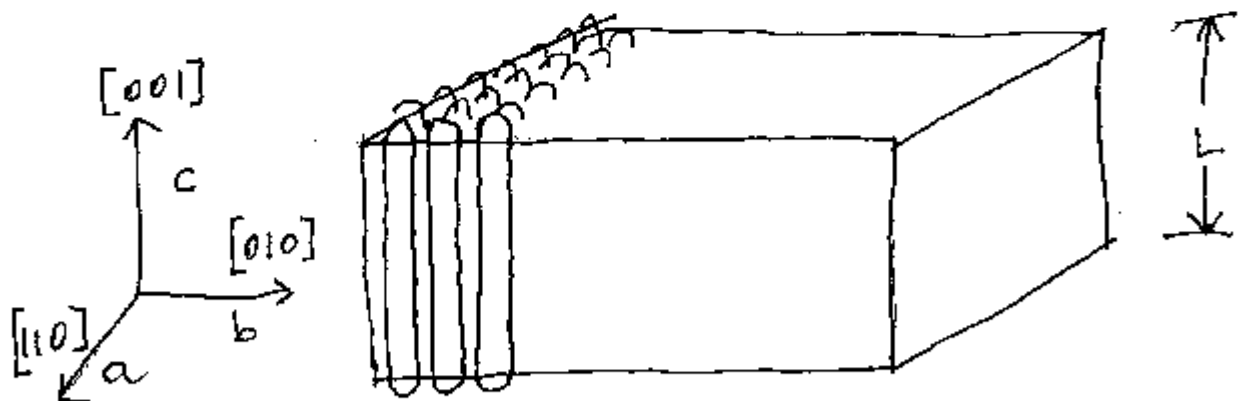
Type	aspect	Typical content in crystalline phase, %	Type of Crystalline defects
Low Density (LDPE)	Opaque white pellets	30	Configurational (chemical end groups)
High Density (HDPE)	white powder	70	Conformational (geometry of catena)

Block morphology : “shish-kebab” = crystalline lamellae randomly distributed in amorphous phase.

Morphology of highly oriented samples (films, yarns): oriented crystalline lamellae.

Lamellar habit :

Orthorhombic unit cell, $T=20^\circ\text{C}$, $p=0.1\text{ MPa}$, $a=7.43\text{ \AA}$, $b=4.94\text{ \AA}$, $c=2.54\text{ \AA}$



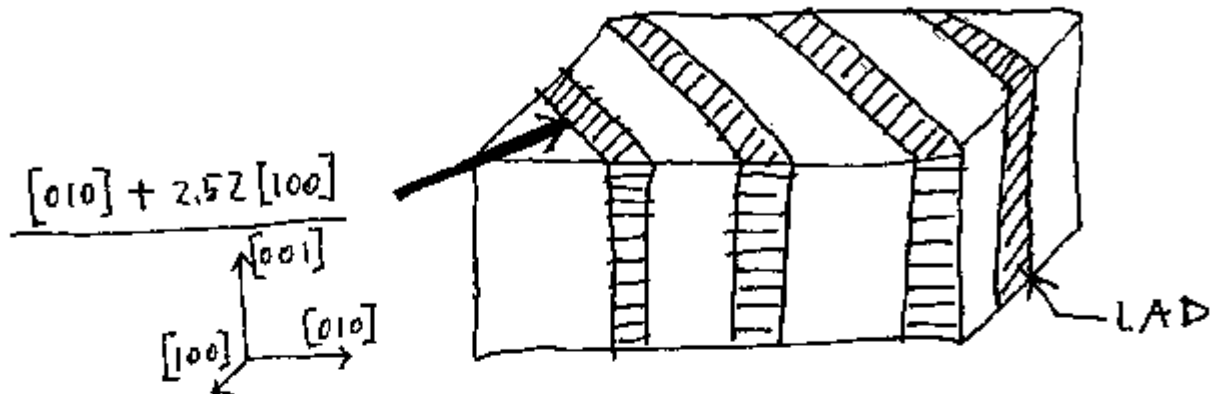
Lamellar thickness (L) :

- usual value approx. 10 nm ;
- after annealing ($100-135^\circ\text{C}$): $\leq 50\text{ nm}$;
- by crystallization from the melt under high pressure : $< 1\text{ }\mu\text{m}$.

(A) (lamellar thickening)

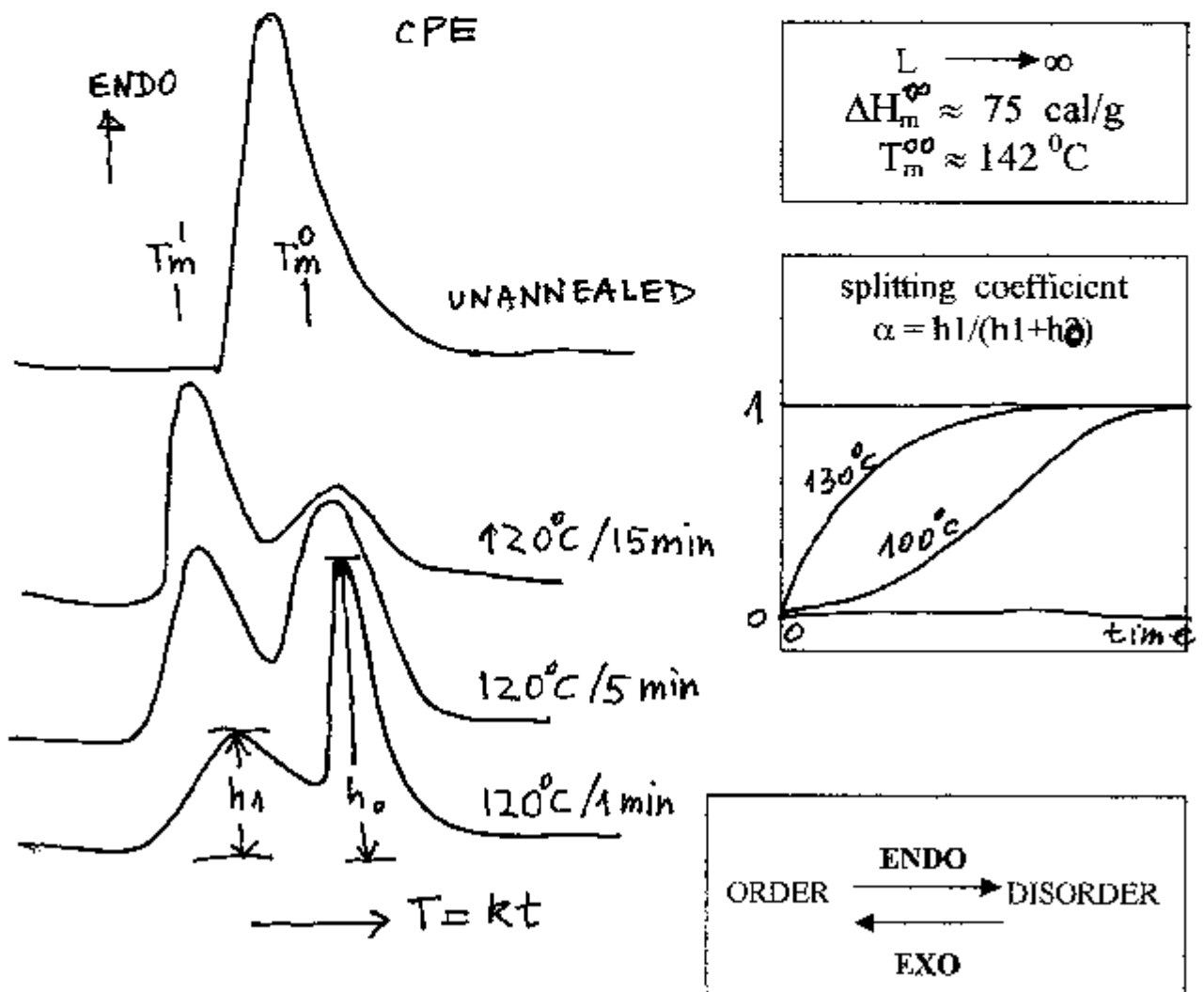
Annealing of LDPE , HDPE with chemically grafted defects

(B) Coherent precipitation of intralamellar defects in Local Amorphous Domains (LAD).



T.Nagasawa & K.Kobayashi, J.Appl.Phys.,41,4276 (1970).

Melting behaviour of PE samples as a function of different treatments :



G.Dragan

Rev.Roumaine Chim.,20,687(1975);28,1315(1981).

J.Polymer Sci.,Polymer Symposium,64,141(1978).

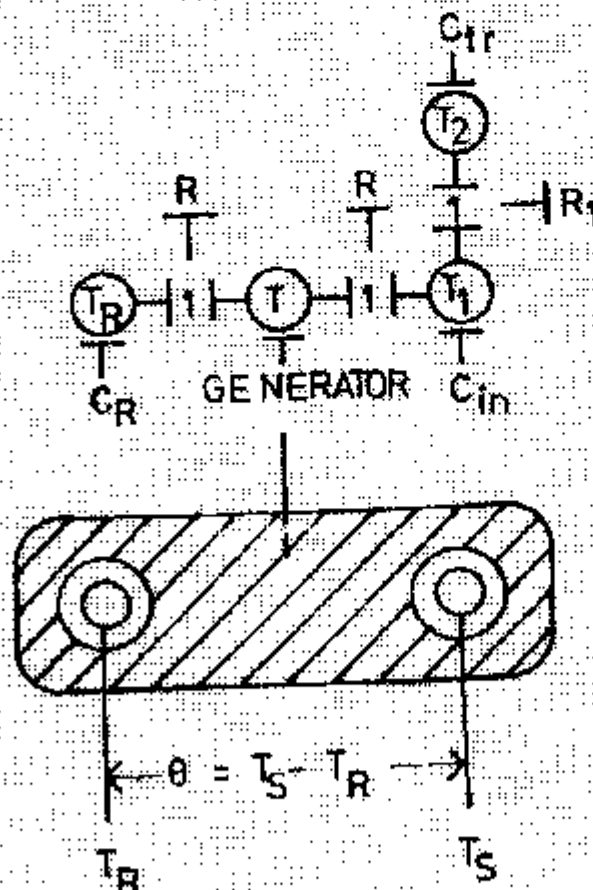
Basic topoenergetic principle:

- energy circuit associated to a system in transformation ~ contribution of components with elementary behavior like in electric circuits (sources, potentials, dissipative, capacitive, inductive, etc.).

G.F. Oster & D.M. Auslander: J. Franklin Institute, 292, 1, 77 (1971)

Differential Thermal Analysis (DTA) Differential Scanning Calorimeter (DSC)

- any system in transformation is a composite system because at least two capacitive components mutually interact.



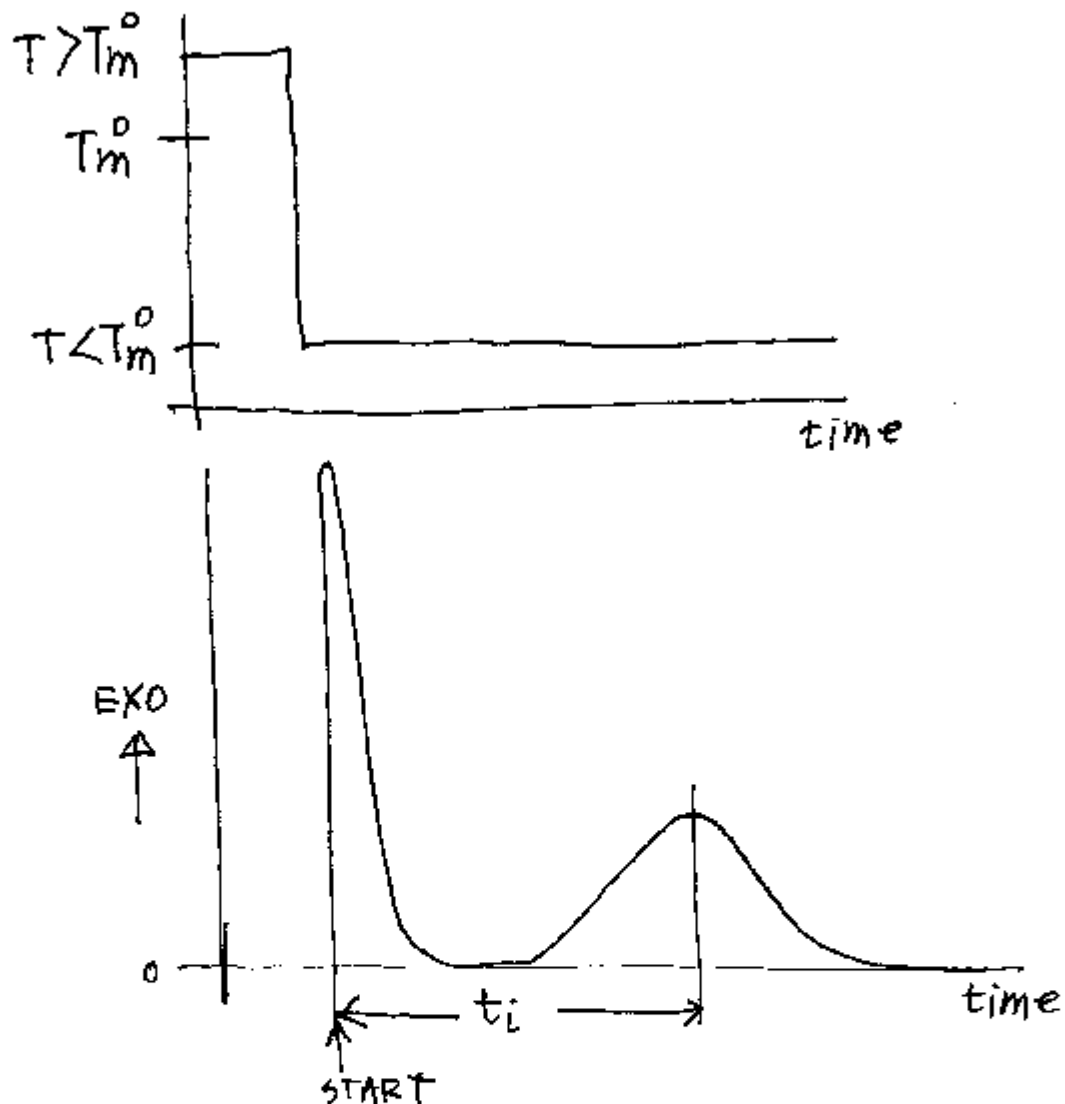
BOND DIAGRAM

PHYSICAL
DISPOSITION

G. Drăgan,
J. Thermal Anal., 9, 405 (1976); 15, 297 (1979).

Processes in the approximation of purely dissipative coupling

HDPE crystallization from the melt.



$$\tau \equiv C_{tr} \cdot R_l = \tau_0 \cdot \exp(-E/(R \cdot T))$$

E = activation energy, R = gas constant

t_i = experimental eigenvalue, T = temperature as driving potential

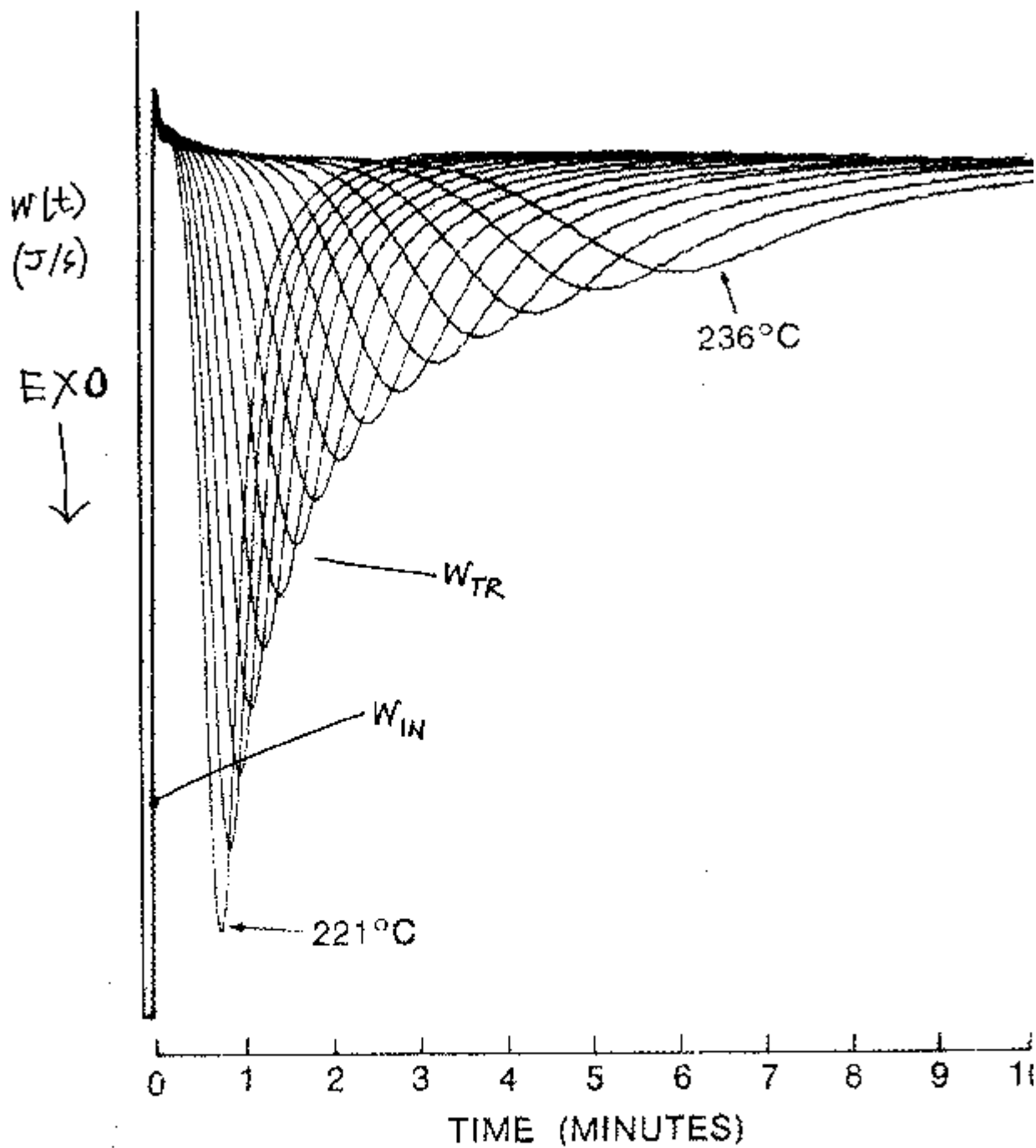
$$\ln(t_i \cdot T) = -E/(R \cdot T) + K$$

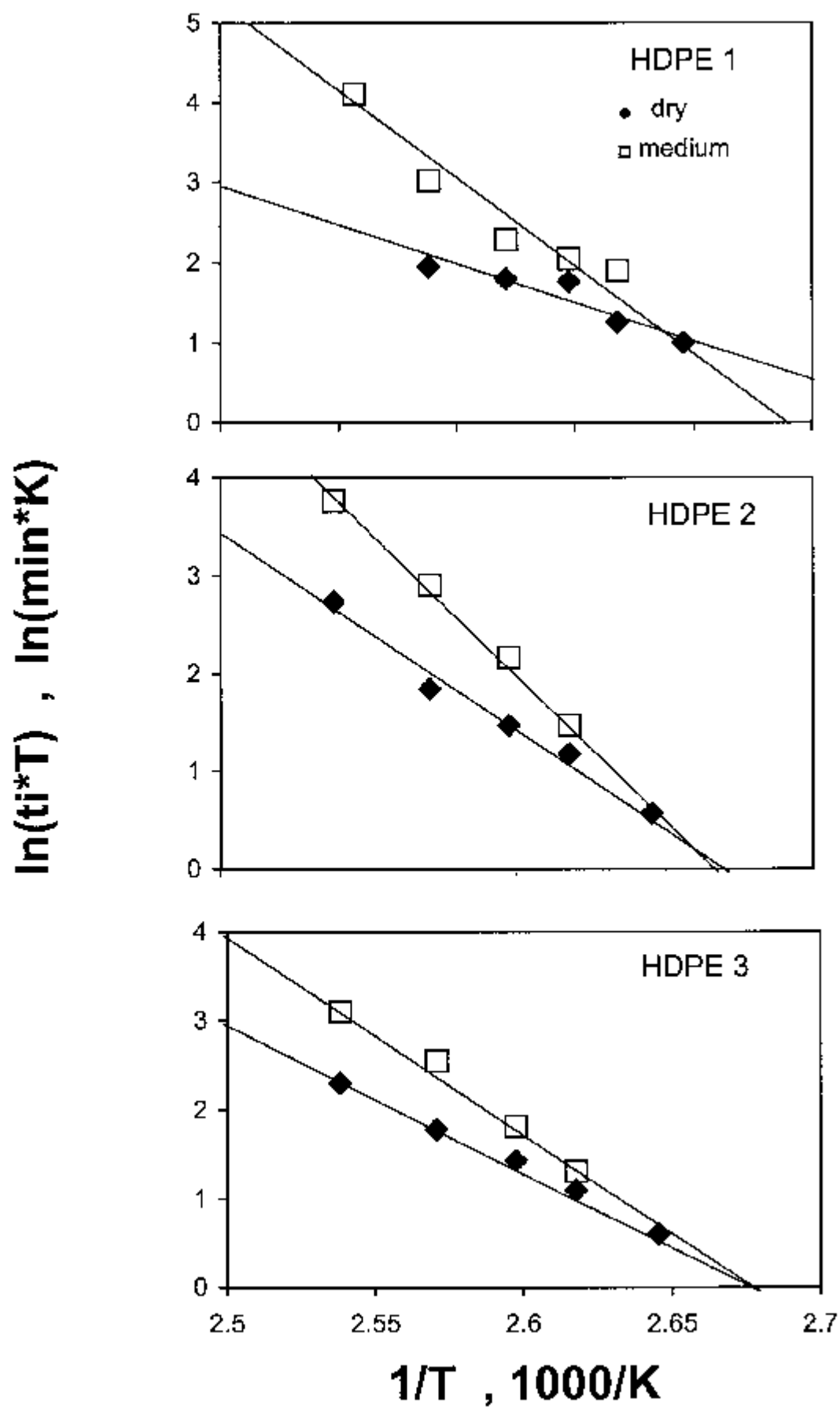
$$K = \ln(C_{tr} \cdot R_l \cdot E/R)$$

(E, K) = define the process in the measuring system

G. Dragan

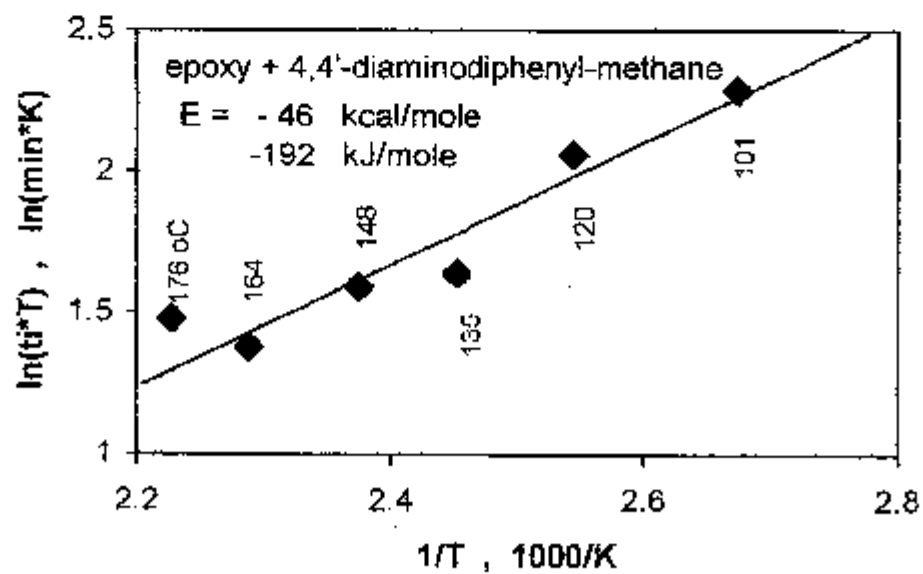
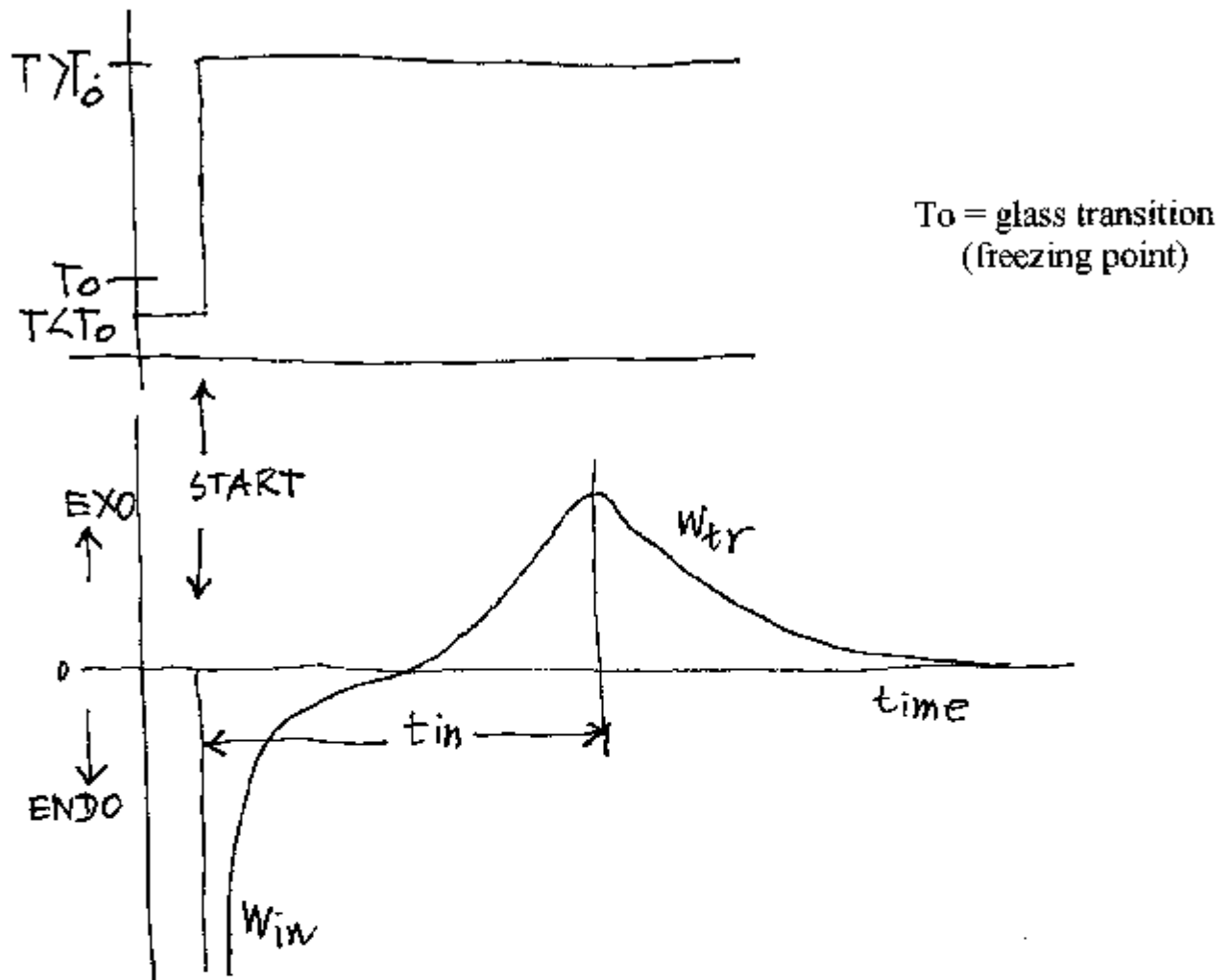
Rev. Roumaine Chim., 23,629(1978).





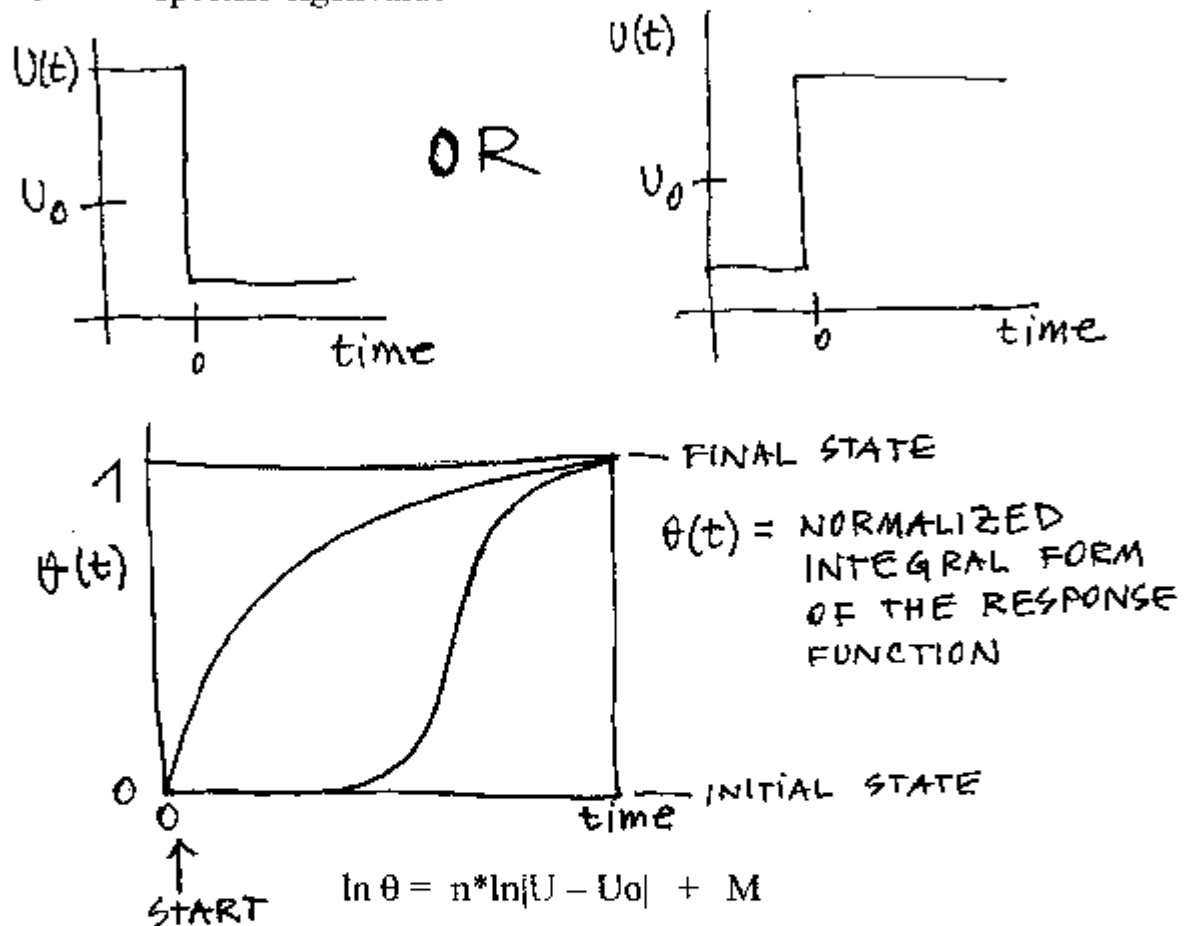
Arrhenius representation of crystallization from the melt for three HDPE brands.

Curing-polymerization of an epoxide resin.



UNIVERSAL Representation of transformation processes

- U - driving potential
- U_0 - threshold value
- $\theta(t)$ - time conversion of the response function
- θ - specific eigenvalue

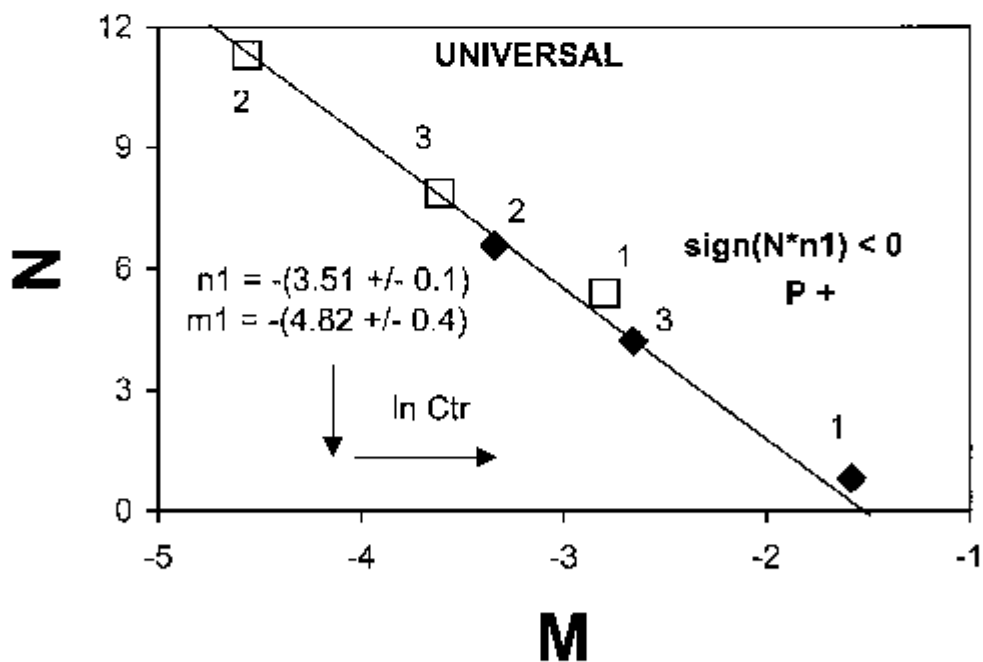
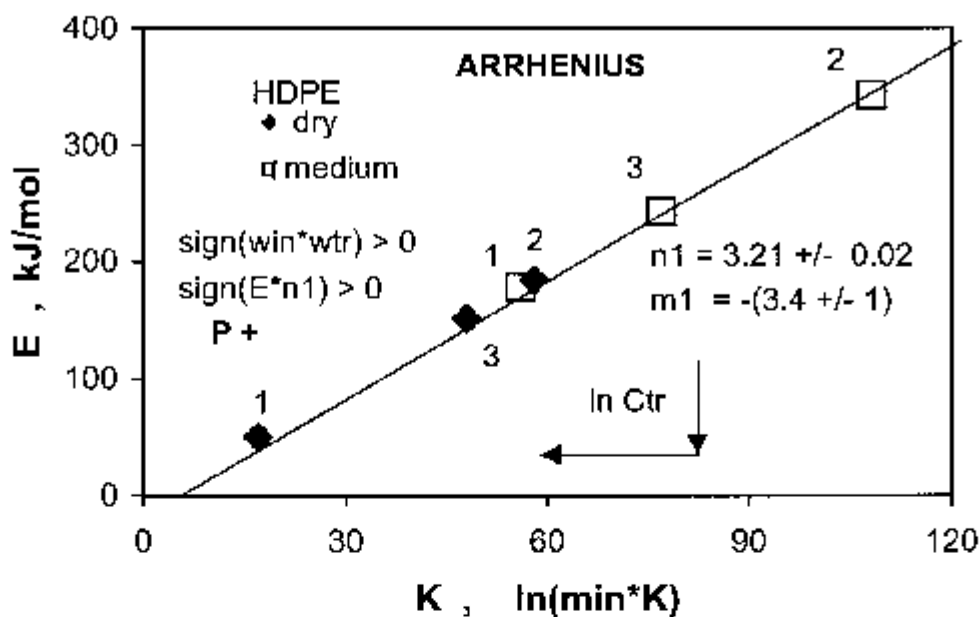


(N, M, U_0) = ontogenic topoenergetic parameters defining the behaviour of a particular sample in a measuring system

For a series of samples with the same transforming process but with different Ctr/Cin ratios :

$$N = n_1 \cdot M + m_1$$

(n_1, m_1) = first phlogenic parameters defining the nature of the transforming process relative to the overall experimental conditions.



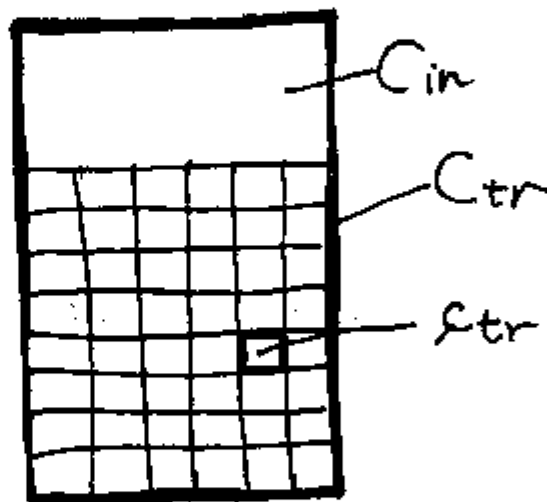
First phylogeny of crystallization from the melt for three HDPE brands in Arrhenius and Universal representations.

Content in crystalline phase : 17372

Standard experimental conditions :

- stepwise variation of driving potential over a threshold value triggering the transformation process;
- good experimental repeatability :
 - the same experimental procedure
 - the same observer (operator)
 - the same measuring instrument
 - the same location
 - repetition/experiments over a short period of time
- volume normalized tested specimens

TESTED SPECIMEN

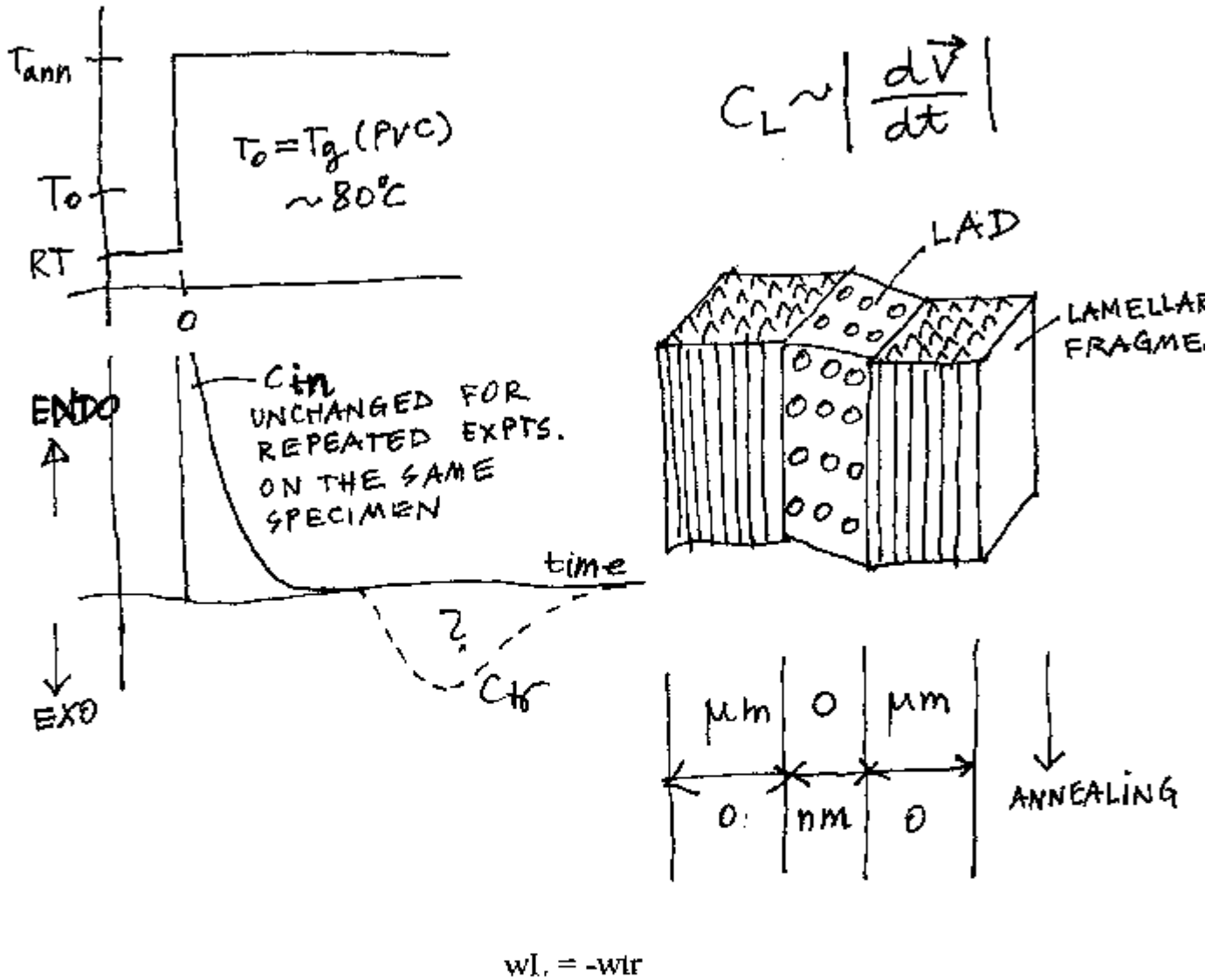


Assignments of kinetic parameters for Arrhenius and UNIVERSAL representations:

Sign(wtr*win)	P	Sign(E*n1)	Sign(N*n1)	M	-M/N	N ² /M	Typical process
+	+	+	-	-lnCtr	-lnctr	CS	Crystallization from the melt
-	-	-	+	lnCtr	lnctr		Polymerization

INDUCTIVE ELEMENT

Annealing of CPE samples in the drop calorimeter (as *in vivo* measuring system)



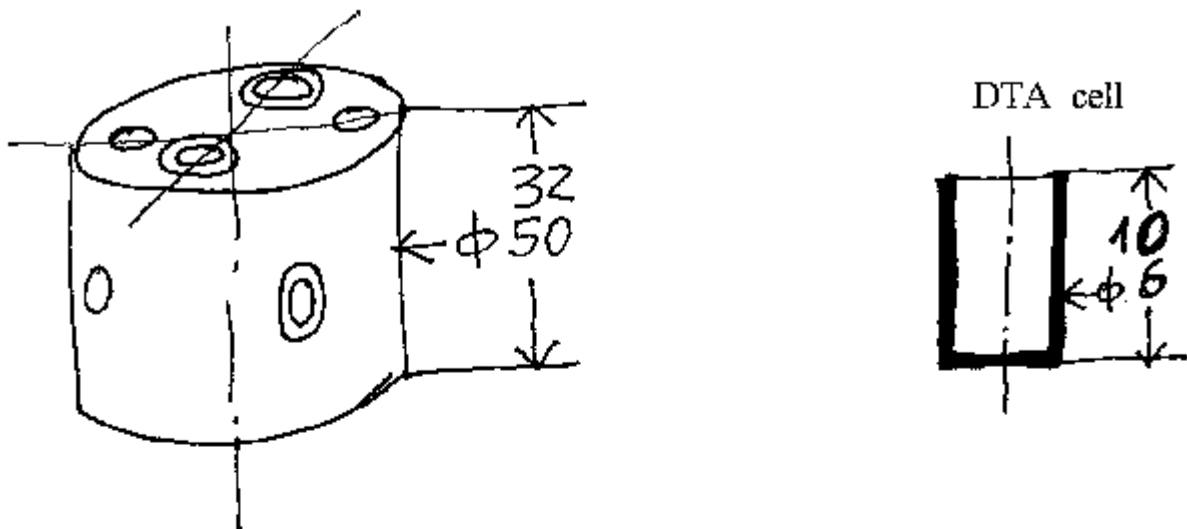
Process of β -decay : $n \longrightarrow p + e^-$

Violation of conservation laws for energy and kinetic momentum evidenced by calorimetric measurements. New particle, or an inductive component?

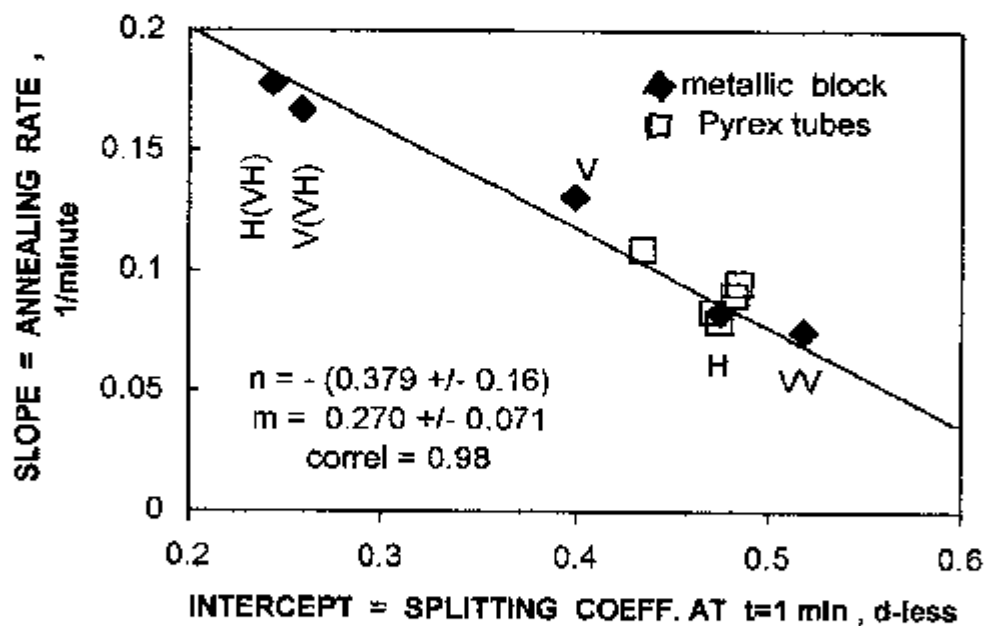
C.D.Ellis & W.A.Wooster : Roy.Soc.Proc., A 117, 109 (1927)

L.Meitner & W.Orthmann : Zeitschrift für Physik, 60, 143 (1930).

Inductive interaction between two simultaneously annealed samples



The brass block used for isothermally annealing of medium samples (CPE+silicon oil) at $131.3 \pm 0.05^\circ\text{C}$.

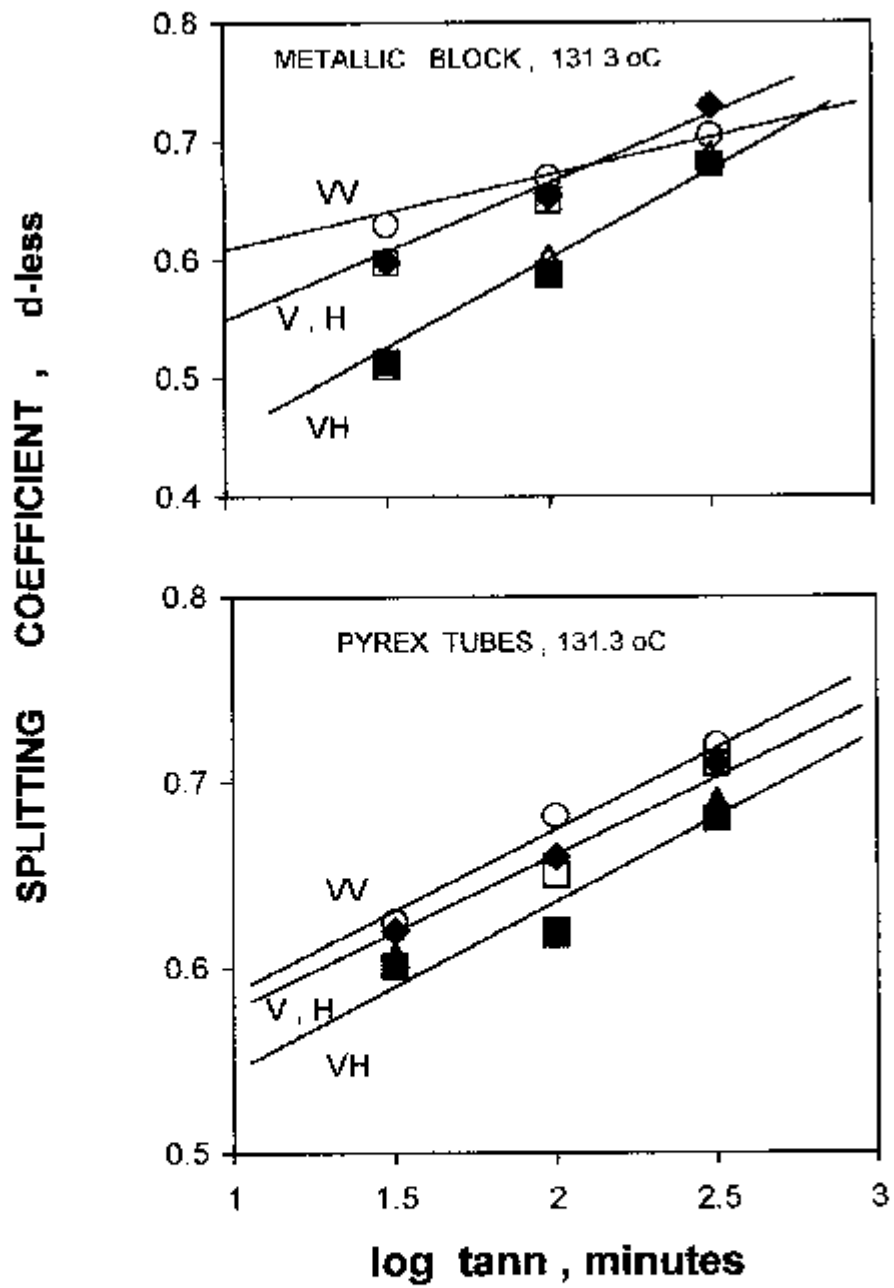


- The amplitude of early stage of defect precipitation (α_0):

$$VV > H > V > H(VH), V(VH)$$

- The rate of defect precipitation at long time ($d\alpha/dt$):

$$VV < H < V < H(VH), V(VH)$$

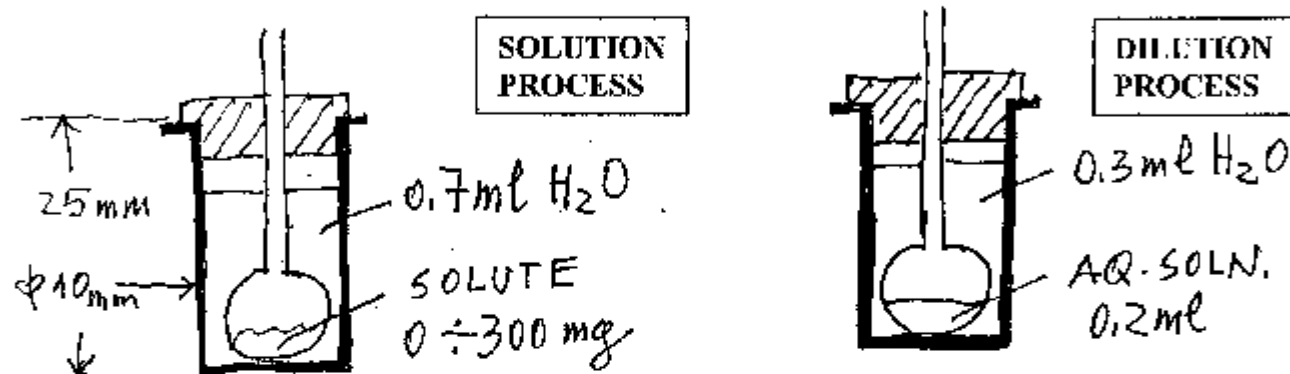
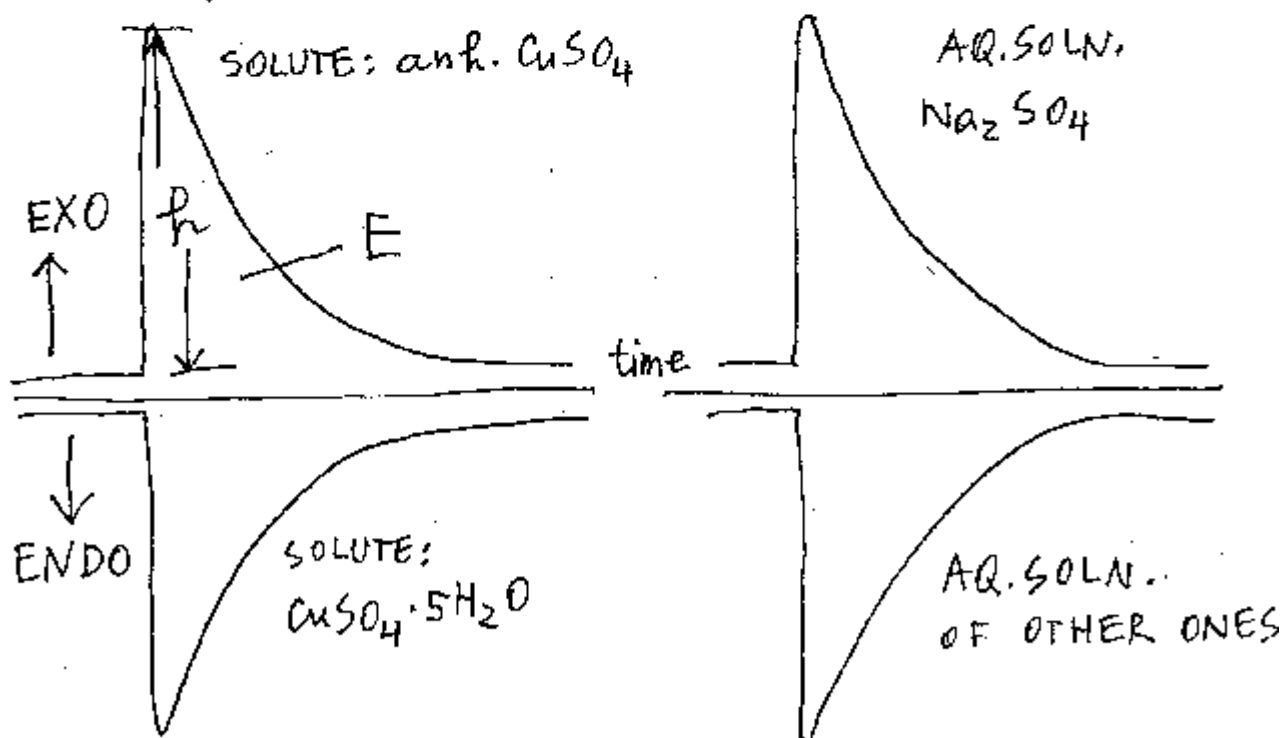


WATER & AQUEOUS SOLUTIONS

Solubility behaviour

SOLVENT	SOLUTE
Liquid water	Solid (ionic salt)
volume (solvent) \gg volume (solute)	

High Resolution Mixing Calorimetry (HRMC) :

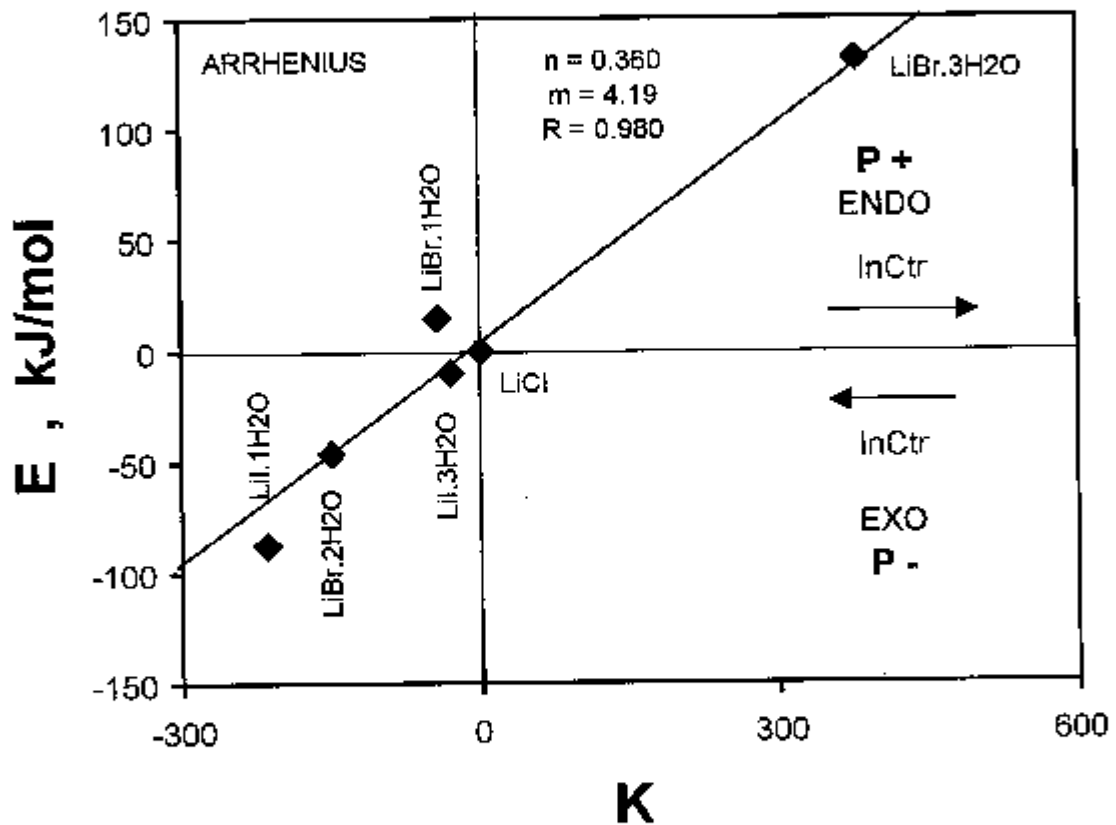
Solute series: $XSO_4 (H_2O)_n$, X : Cu, Na₂, K₂, Mn, Fe, Ni, Mg.

G. Dragan

J. Thermal Anal., 31, 677; 941 (1986); 32, 293 (1987).

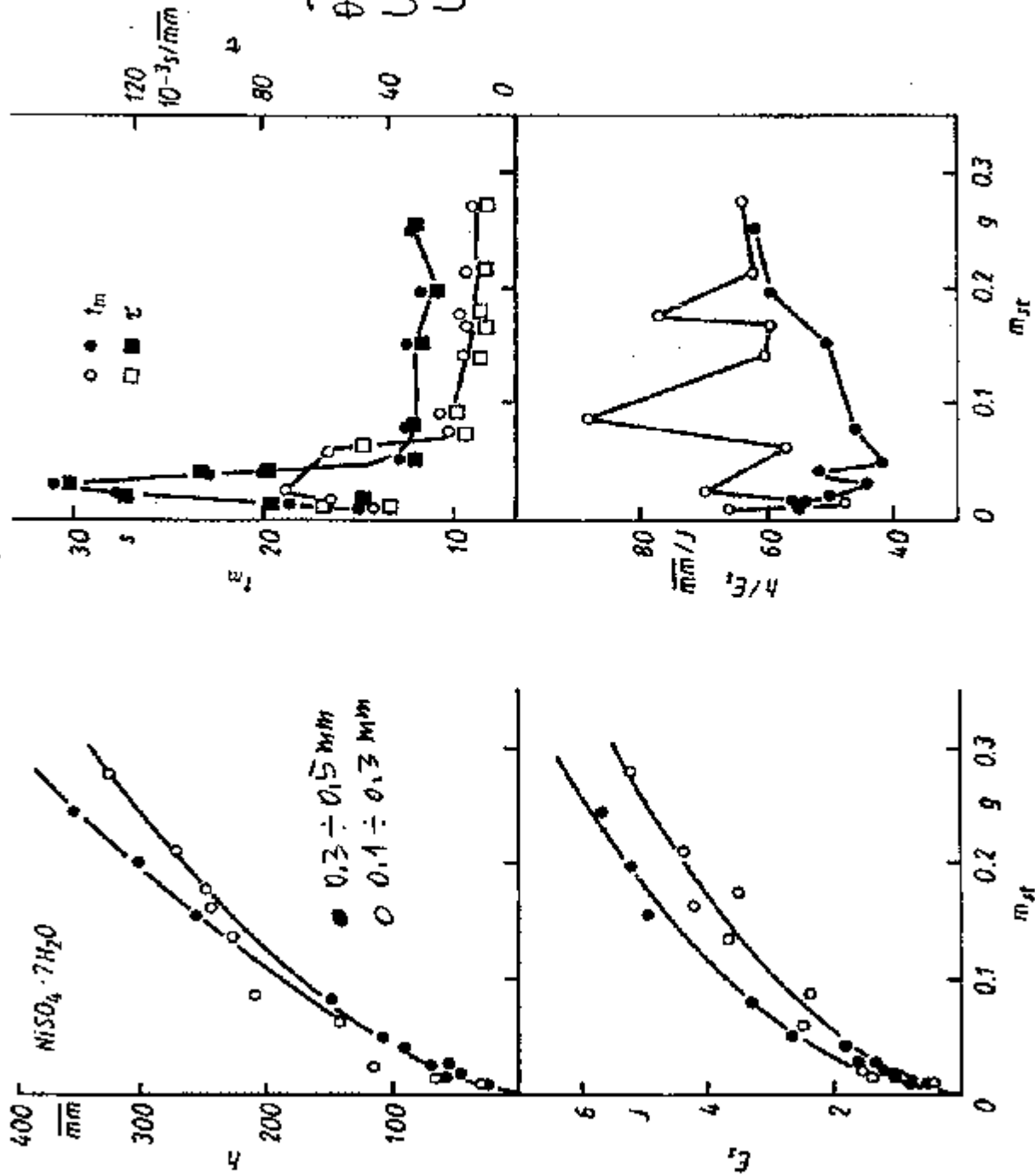
teta = [anh. salt]eq , (g anh.salt/g water)

U = temperature (oC)



experimental data from :

M.Broul, J.Nyvt, O.Sohnel, "Solubility in inorganic two-component systems", Academy, Prague, 1981.



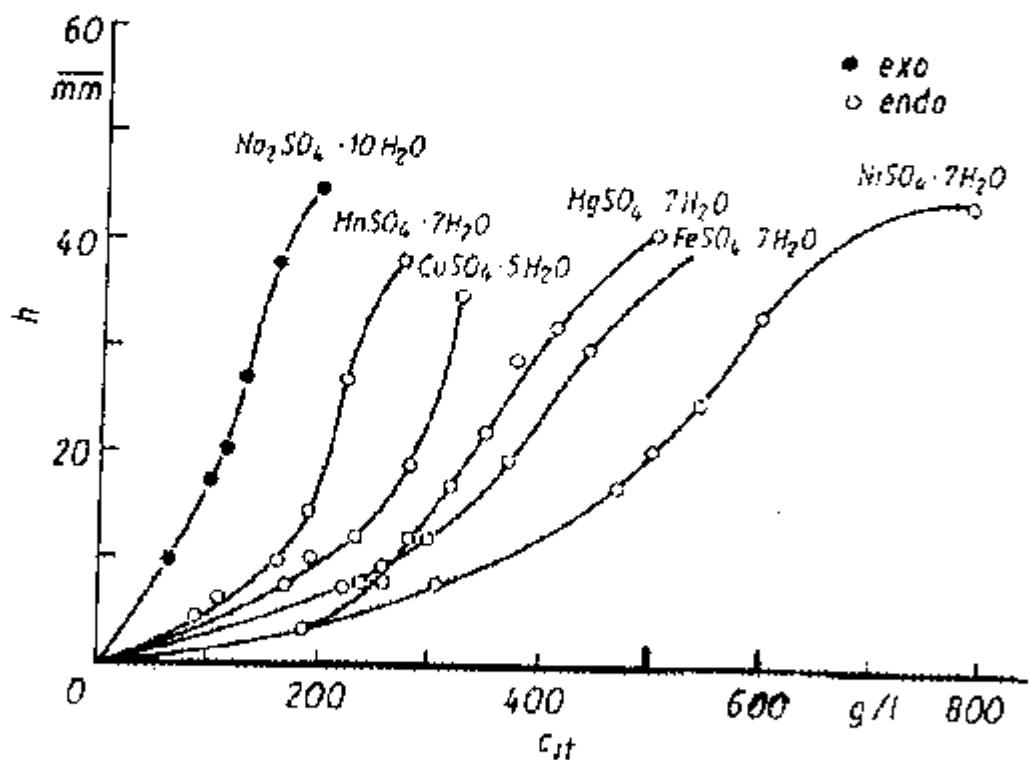
The dependence of the five IIRMC parameters on m_d , determined for the solution of two grain size fractions of $\text{NiSO}_4 \cdot 7\text{H}_2\text{O}$ in standard test specimens

DILUTION PROCESS

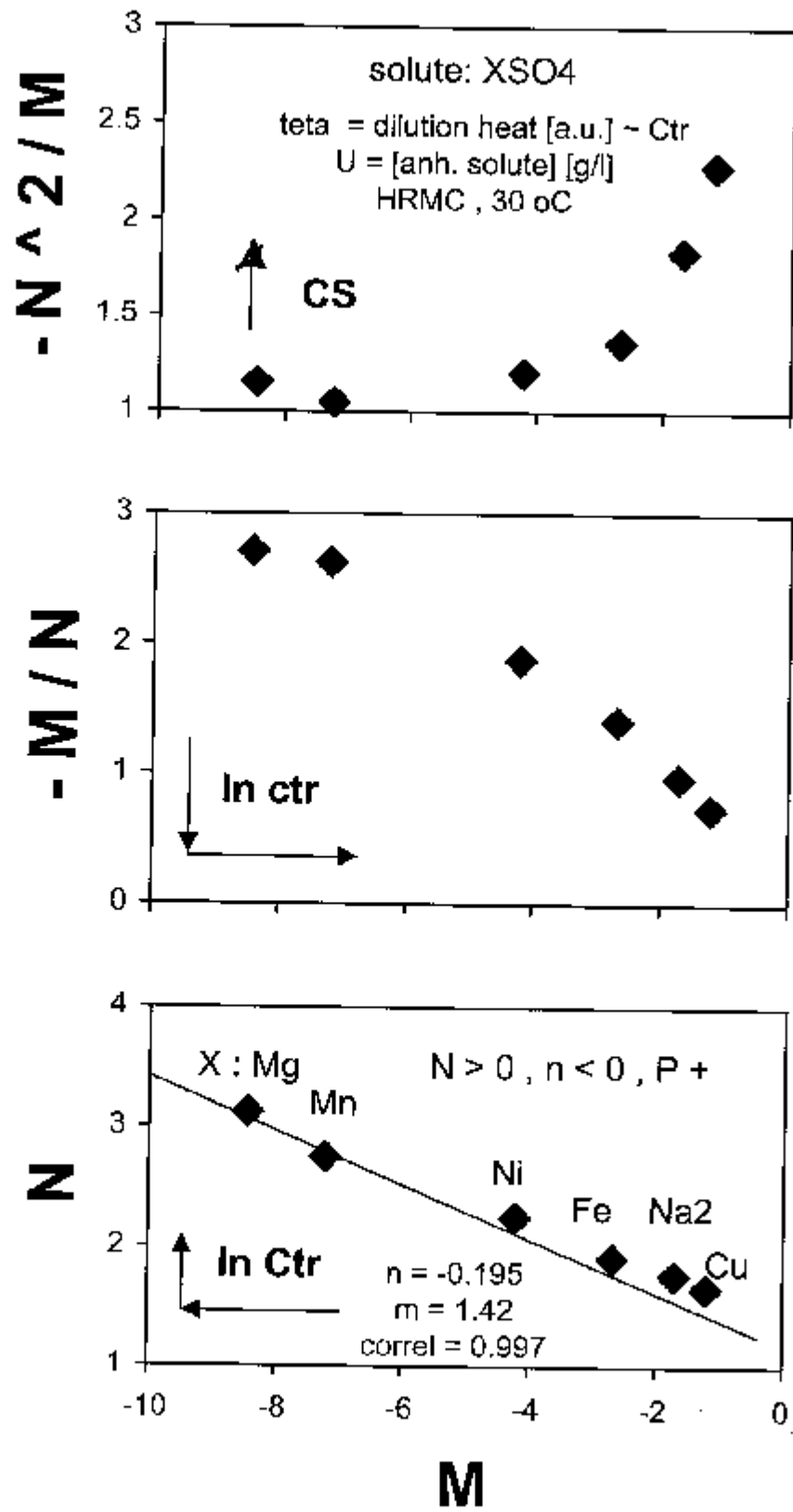
$$\theta = h_d ; E_d$$

$$U = [\text{anh. solute}], [\text{g/l}]$$

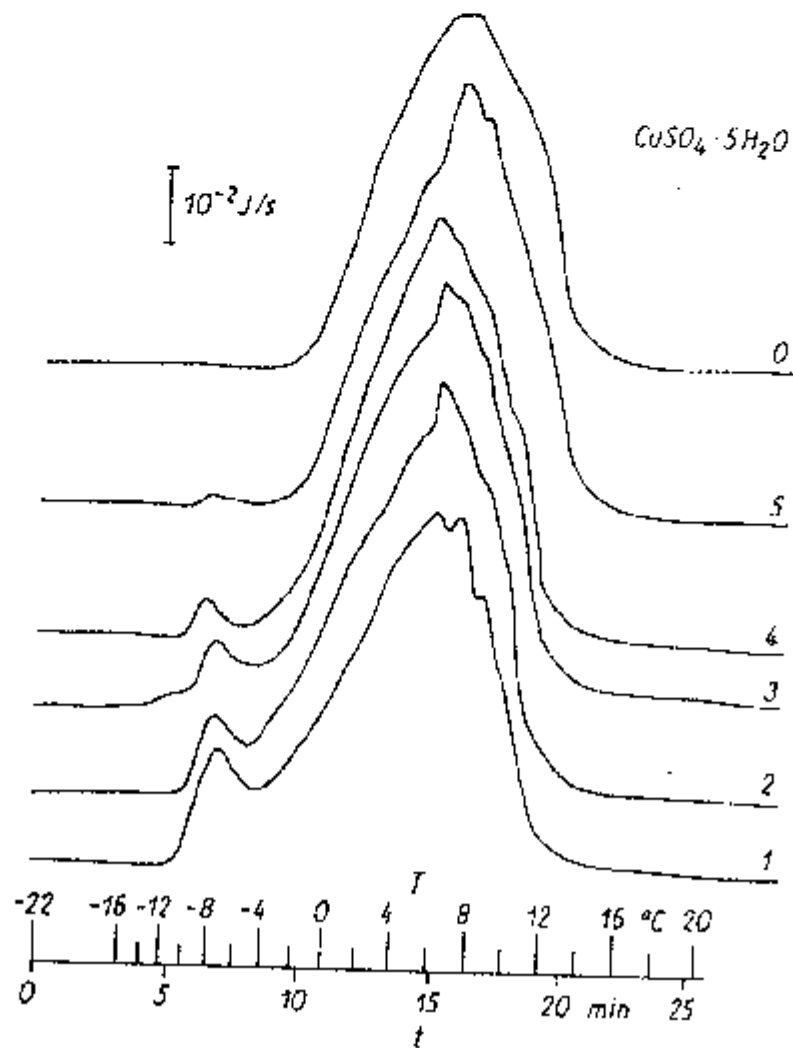
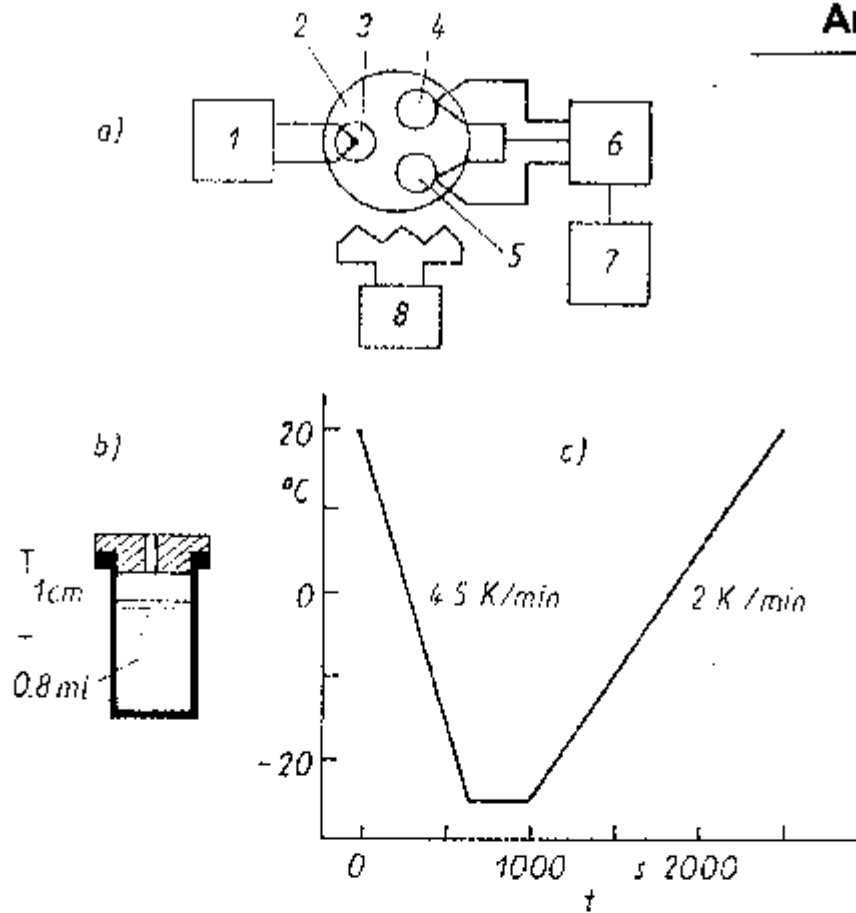
$$U_0 = 0$$



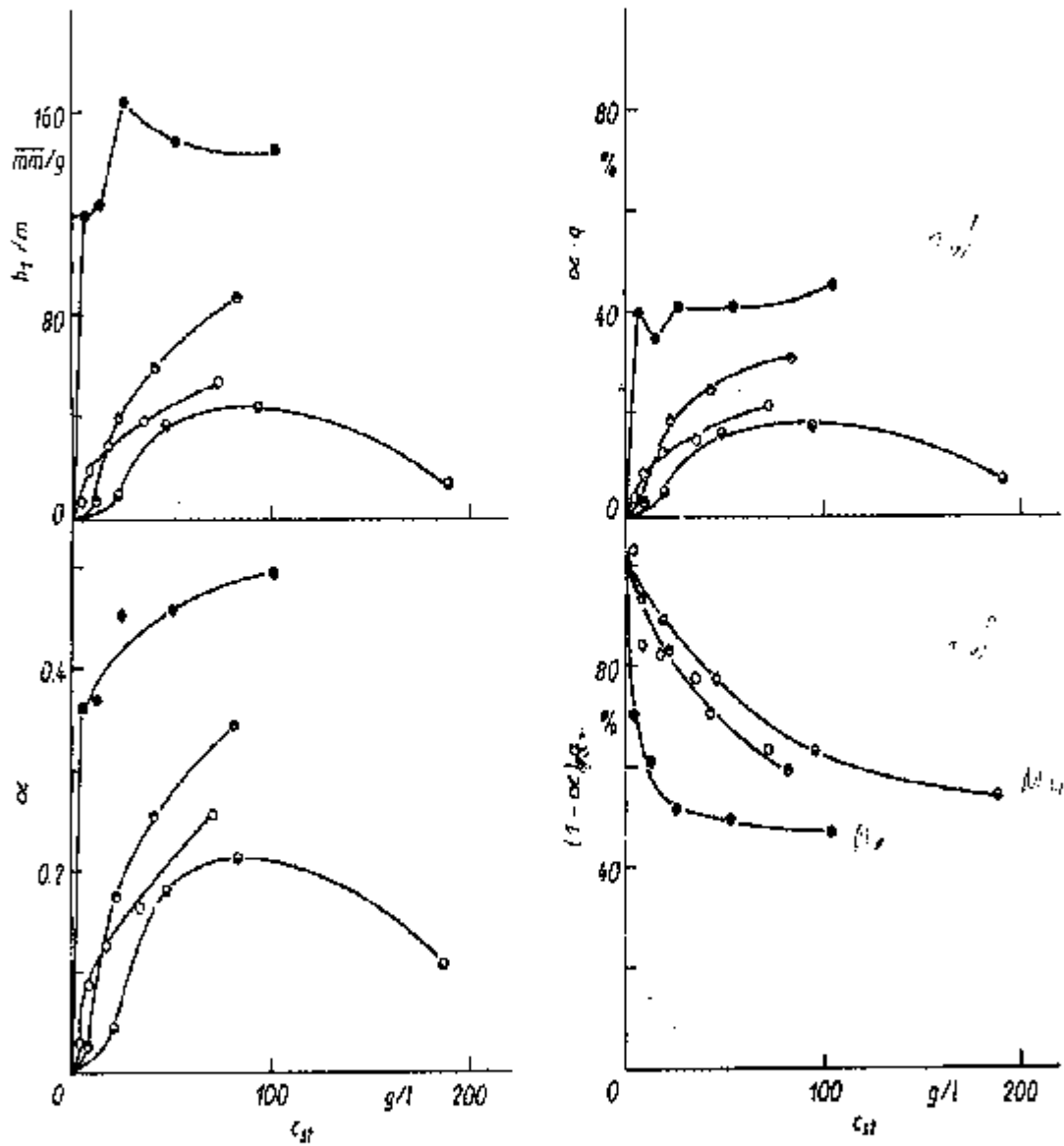
Dependence of peak height on solution concentration (mass of solute without crystal water) of several hydrated sulfates diluted at $26.2^\circ\text{C} \pm 0.6$ by HRMC



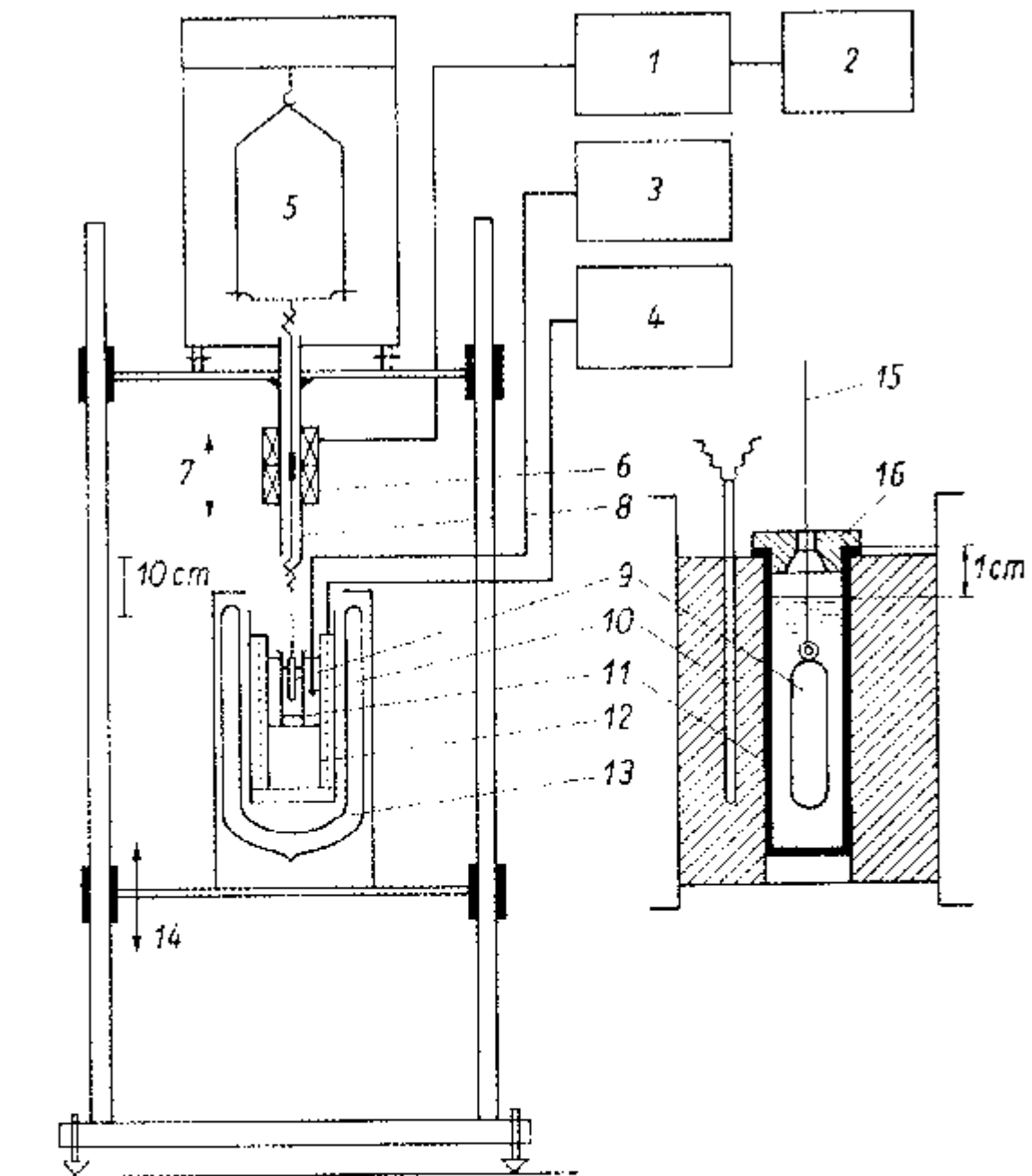
Topoenergetic representation of dilution process of XSO₄.



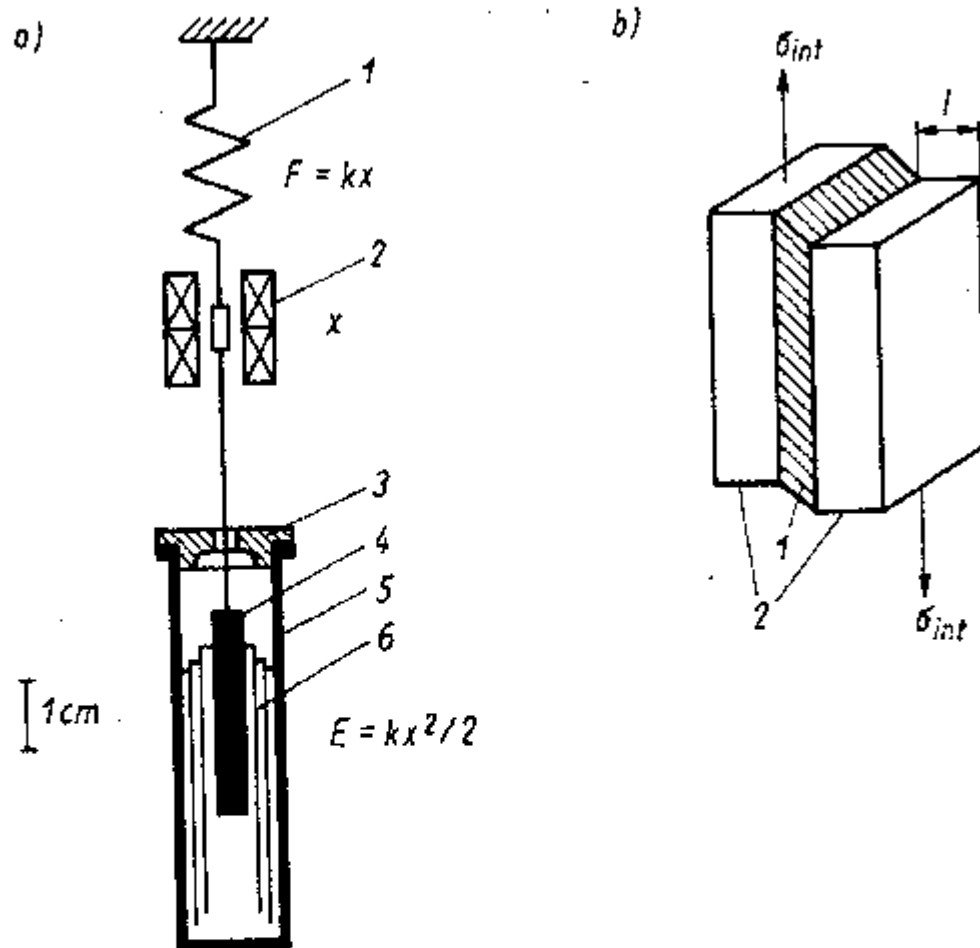
DSC melting endotherms of aqueous solutions of $\text{CuSO}_4 \cdot 5\text{H}_2\text{O}$, successively diluted to half concentration. 0 — pure



Dependence of c_H of four selected parameters measured from the DSC melting endotherms for aqueous solutions of CuSO_4 (\circ), NiSO_4 (\square), MnSO_4 (\triangle) and Na_2SO_4 (\bullet)

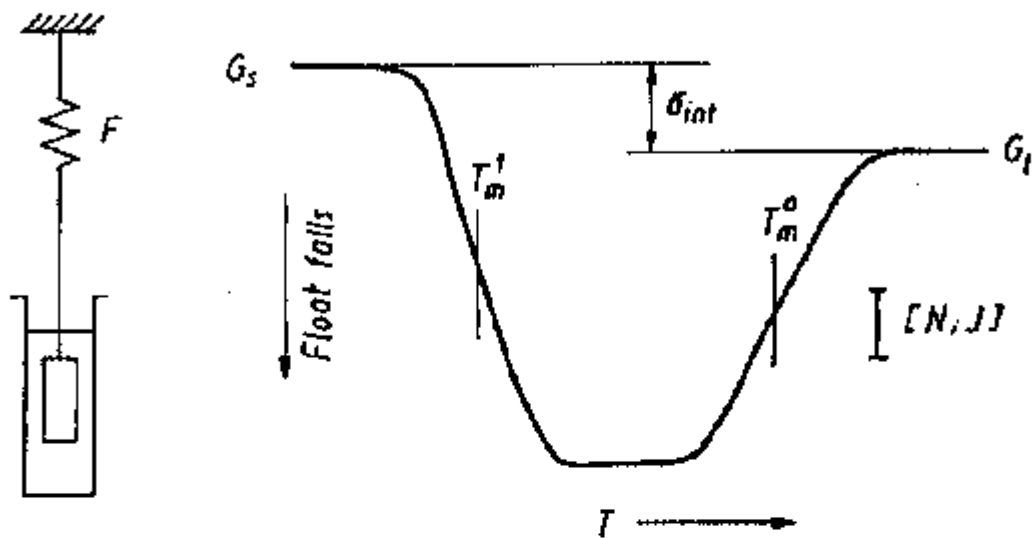


Basic disposition of DFDA and TMA experiments with aqueous solutions. 1 - ac-bridge, lock-in amplifier with digital display; 2 - recorder; 3 - digital Ohm-meter for temperature control (± 0.02 K); 4 - dc-generator for constant heating rate (50 V); 5 - automatic analytical balance (± 0.1 mg); 6 - linear differential transformer for displacements (LDTD) of the ferro-magnetic core connected between the balance and float or plunger; 7 - mechanical adjustment of zero by shifting of LDTD; 8 - protective glass tube; 9 - float or plunger; 10 - thermistor; 11 - cylindrical brass block with the stainless steel pan containing the test sample; 12 - non-inductively coiled heater resistance; 13 - Dewar flask; 14 - sliding support for sample replacement; 15 - cold drawn steel wire ($d = 0.1$ mm); 16 - rubber stopper to avoid freezing of the condensed water

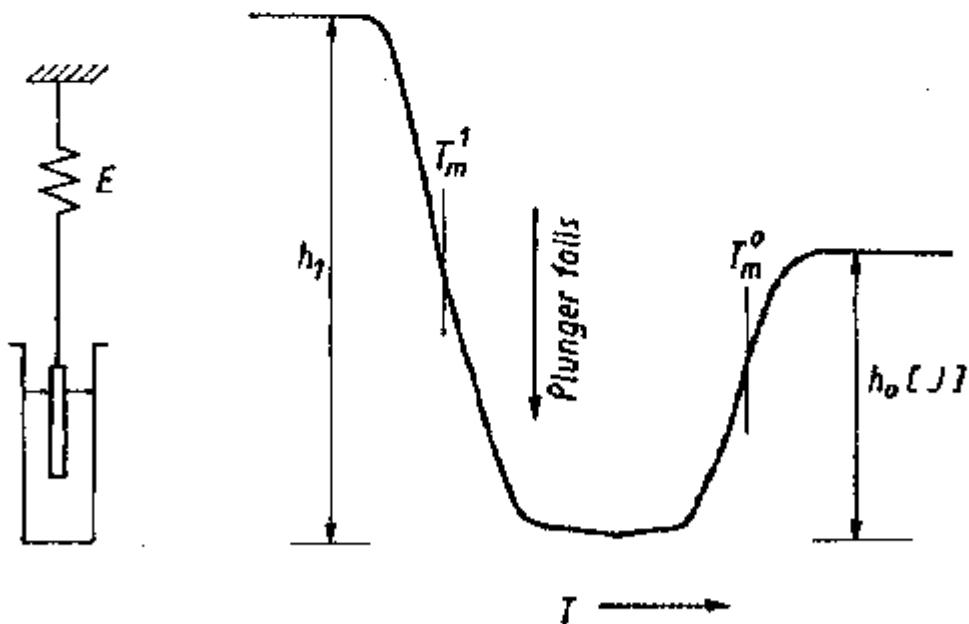


a) Detailed view of the cross-section of the TMA displacement. 1 — elastic element (analytical balance); 2 — LTDT; 3 — rubber stopper for avoiding water condensation from atmosphere; 4 — plunger made from perfectly cylindrical capillary Pyrex glass with 5 mm exterior diameter and 30 mm length (through its axial hole of $d = 0.2$ mm is introduced a cold-drawn steel wire of the same diameter for connection to LTDT); 5 — sample container made from stainless steel; 6 — schematical drawing of the frozen aqueous solution by telescopic cores lifting the plunger. b) Schematical drawing of the intercrystalline precipitate (1) and the crystalline domains (2) with thickness l and accumulating by rapid freezing shear stresses σ_{int}

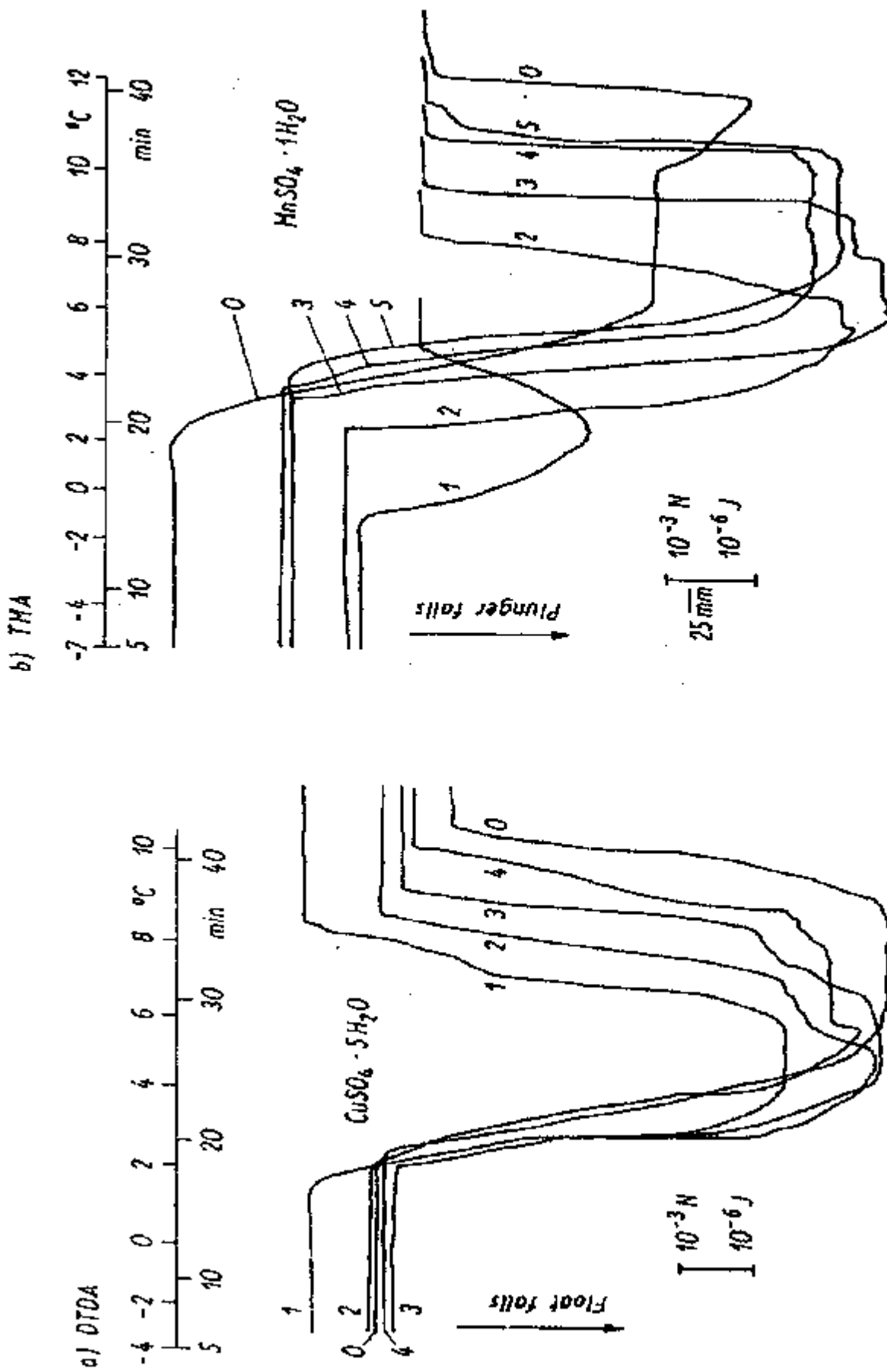
DTDA



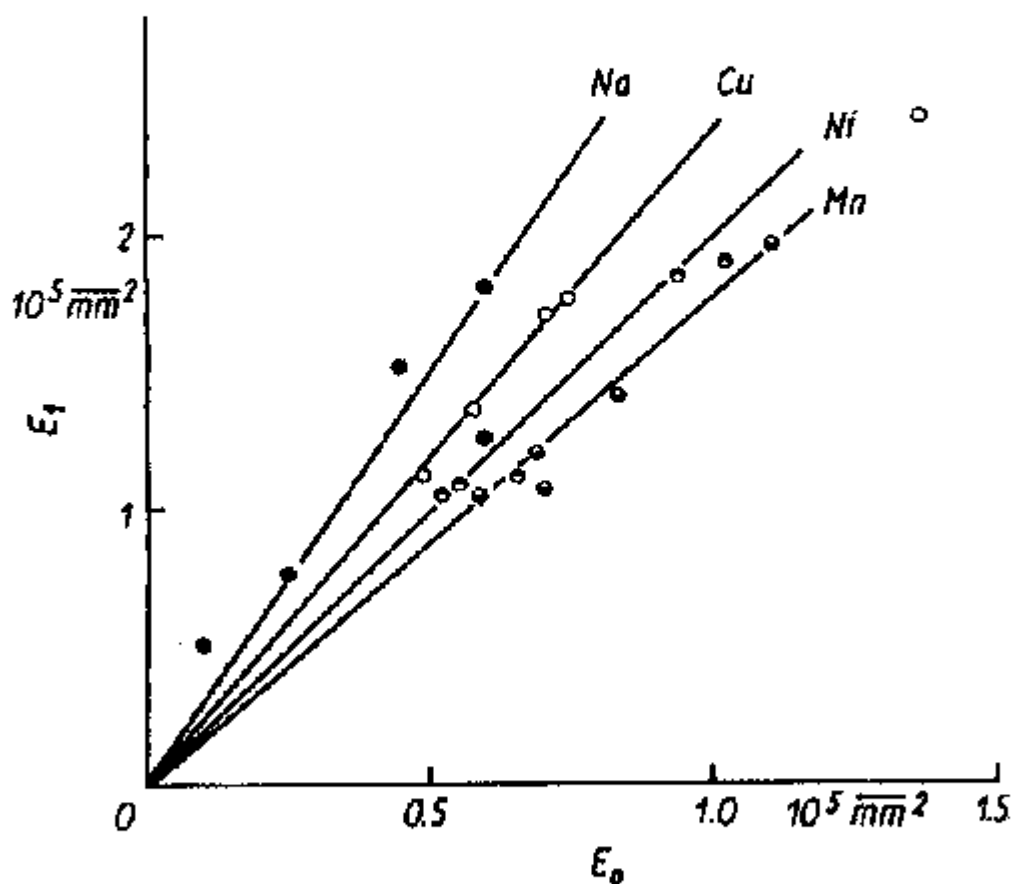
TMA



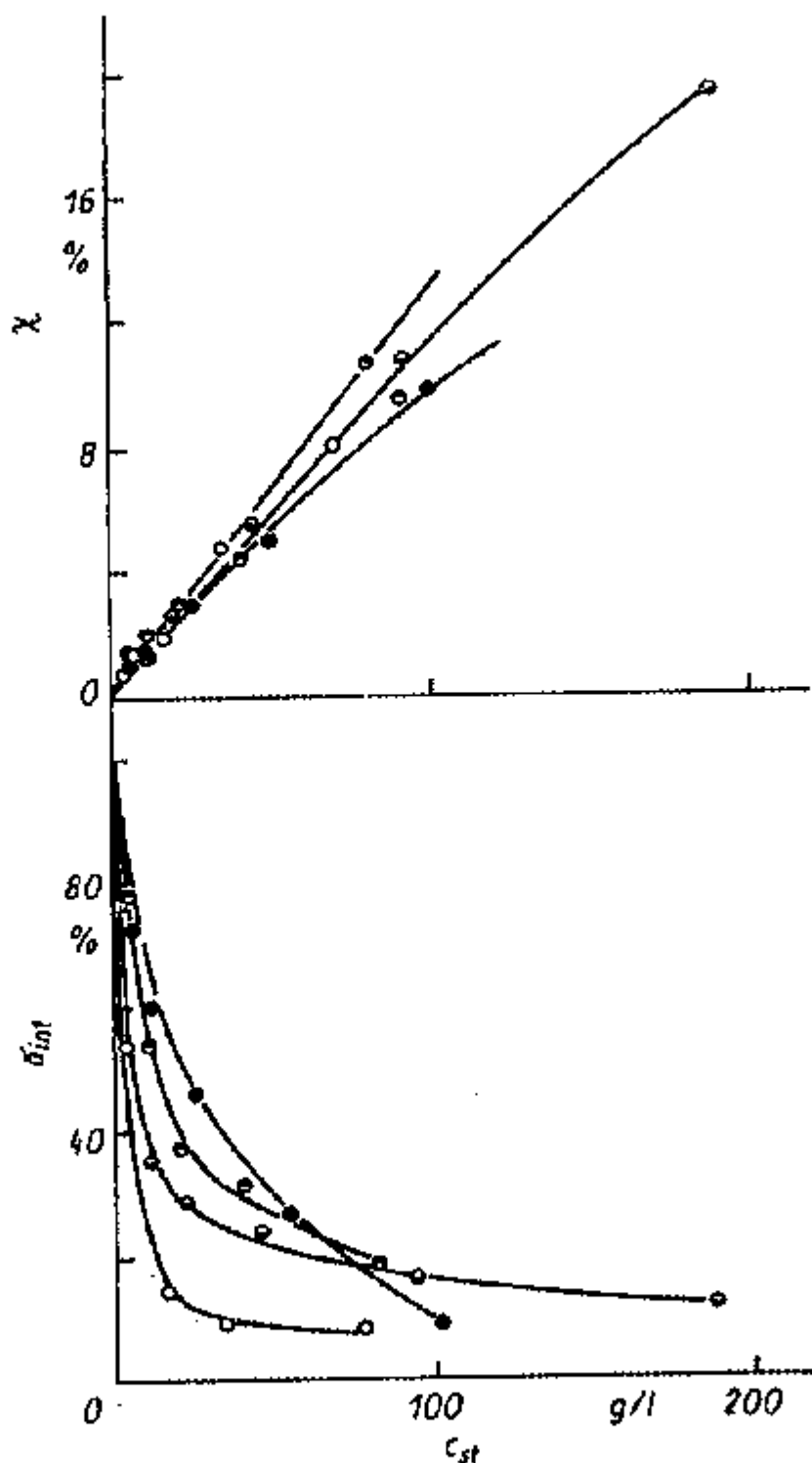
Schematical drawing of the DTDA and TMA techniques and the significance of their associated thermograms (see text)



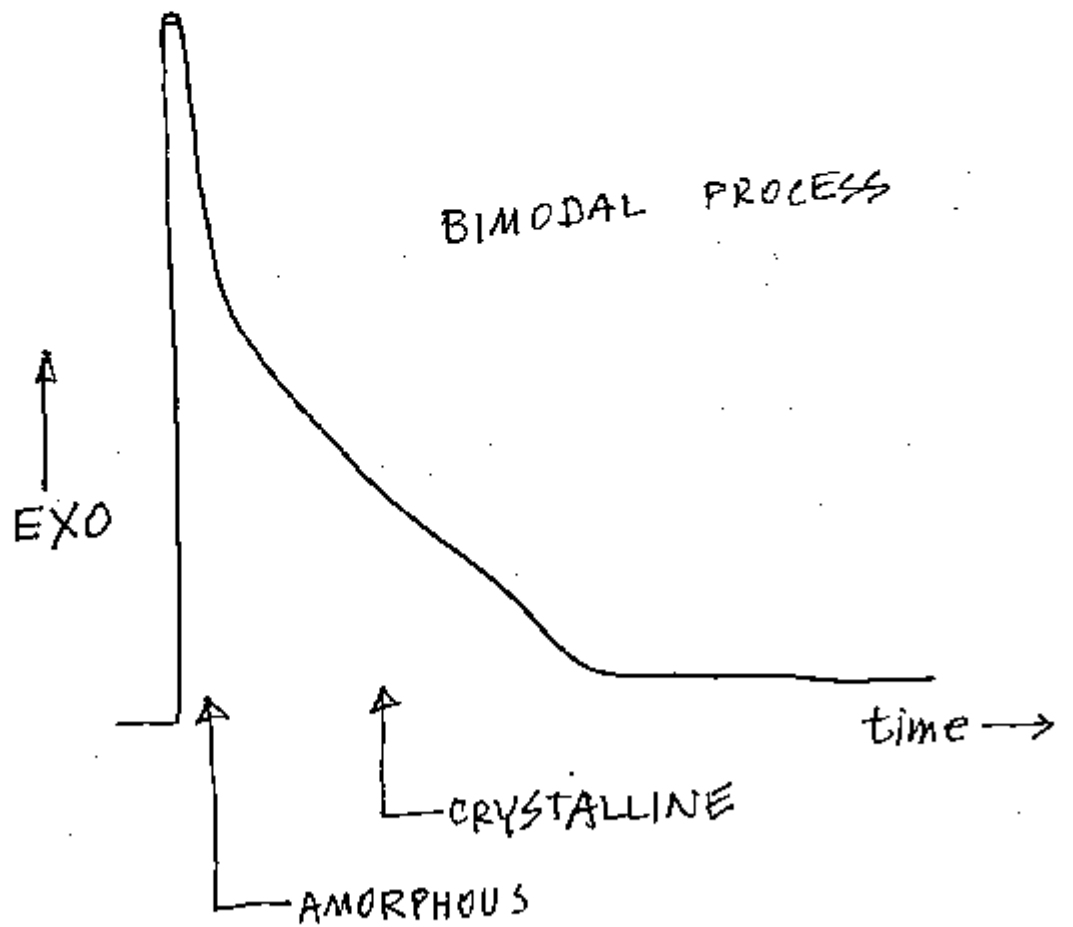
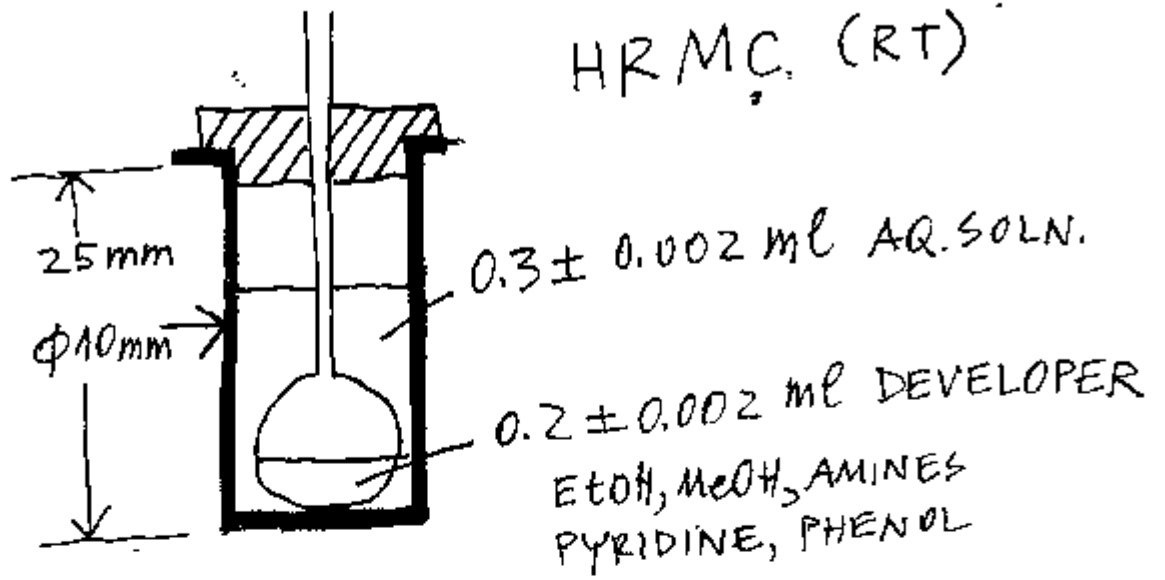
a) DTDA thermograms of representative aqueous solutions successively diluted to half concentration from the initial solution. 0 — pure water; 1 — $\text{CuSO}_4 \cdot 5\text{H}_2\text{O}$, 72.3 g/l (anh.). b) TMA thermograms of representative aqueous solutions successively diluted to half concentration from the initial solution. 0 — pure water; 1 — $\text{MnSO}_4 \cdot 1\text{H}_2\text{O}$, 189.2 g/l (anh.)



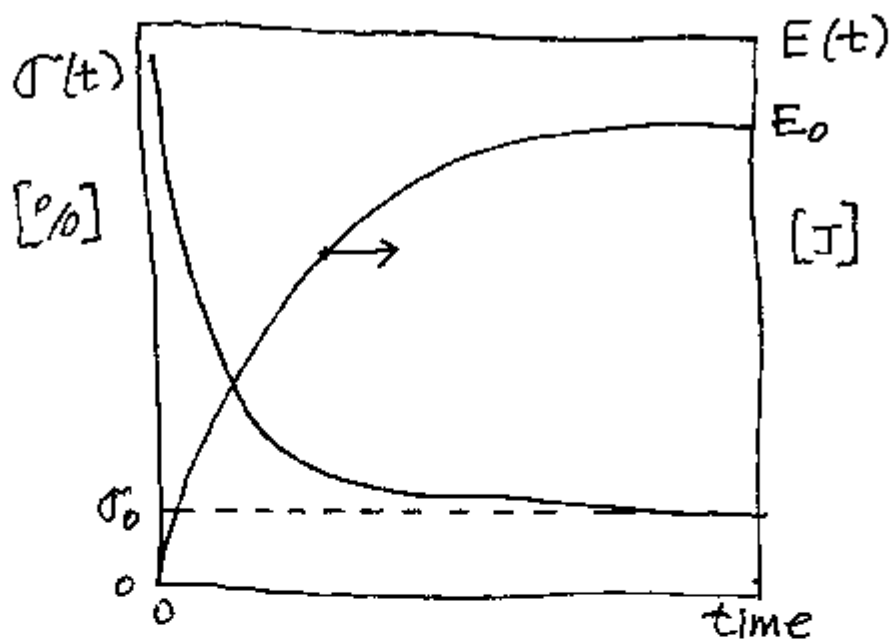
Correlation of the energy associated with T_m^1 intercrystalline order (E_1) and the energy associated with T_m^0 crystalline order (E_0) as determined from TMA diagrams for aqueous solutions of CuSO_4 (○), NiSO_4 (●), MnSO_4 (●) and Na_2SO_4 (•)



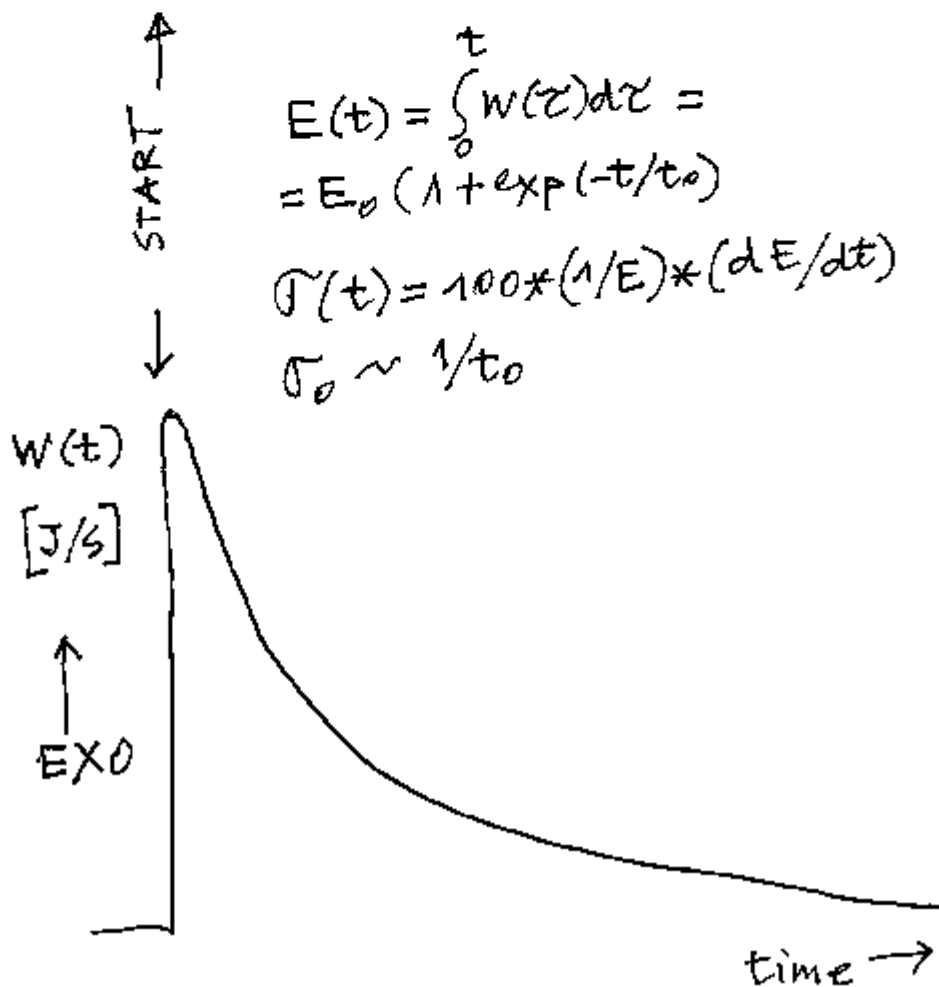
Dependence of σ_{int} and $\chi = [e_t(c_{st}) - e_t(0)]/e_t(0)$ on c_{st} , determined from DTDA thermograms of aqueous solutions of CuSO_4 (\circ), NiSO_4 (\bullet), MnSO_4 (\ominus) and Na_2SO_4 (\cdot)



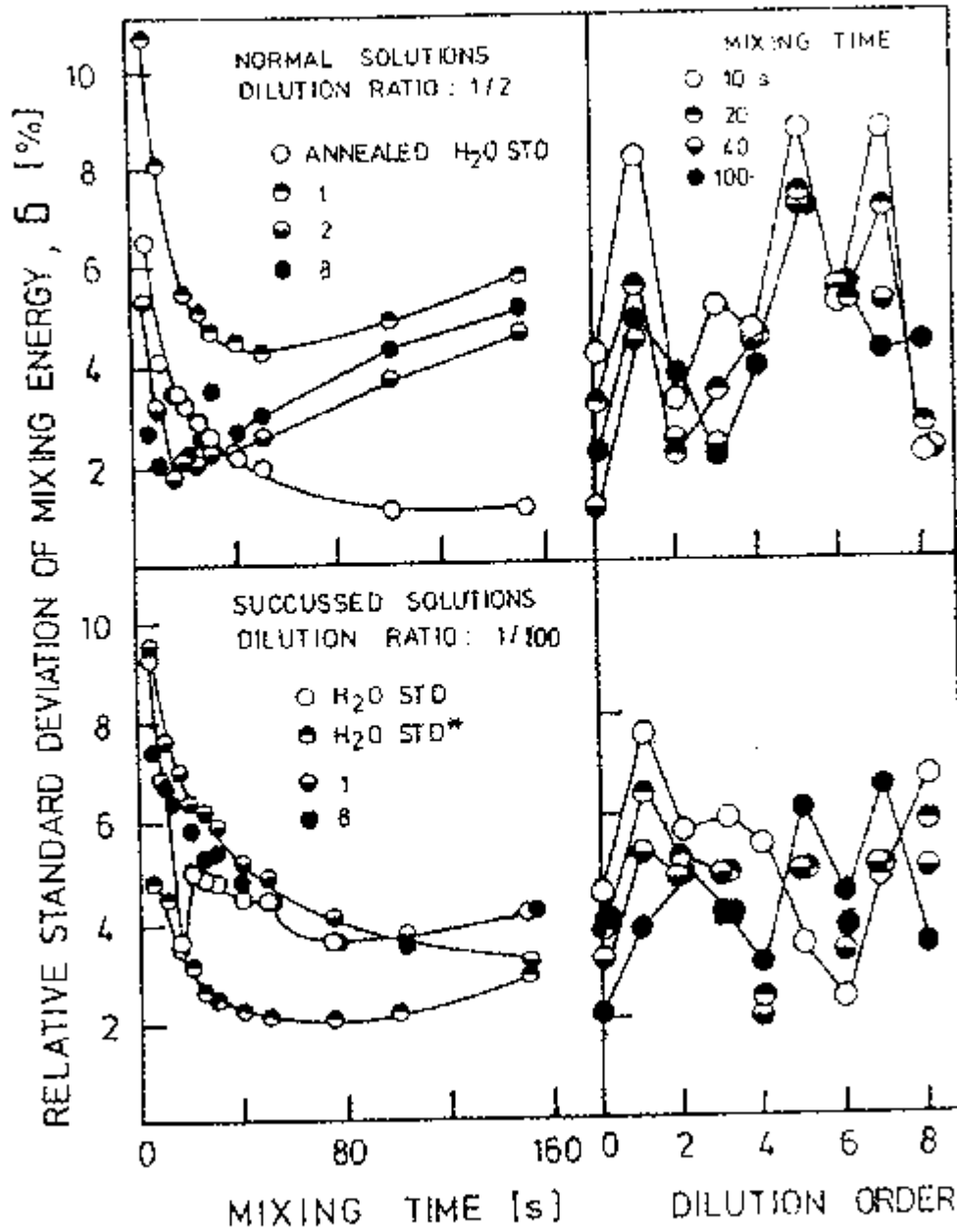
UNIMODAL PROCESS



(a)



(b)



Representation for the relative standard deviation values of the integral mixing energy as a function of mixing time and dilution order for the two series of successively diluted solutions of $Na_3PO_4 \cdot 12H_2O$

HOMOEOPATHY = Samuel HAHNEMANN (1755 – 1843)

- Born in 1755, Meissen (north of Dresden)
- Scholar of Saint-Afra school
- Student of Medicine Faculty in Dresden
- Invited by count Brukenthal at his estate in Sibiu (Romania) as superintendent
- Learns old greek and latin languages, reads Hippocrattes and other ancient scriptures on medicine and philosophy
- Visited India
- Doctorate Thesis at University of Erlangen
- 1791 member of Economic Society from Leipzig and Academy of Mayence
- 1795 settled in Leipzig – brilliant medical activity and social position
- in short time becomes disappointed by medical practice and its inefficiency ; interrupts his medical activity
- begins as copyist and translator
- 1792 publishes :“The friend of health” (Frankfurt)
- translates “Materia Medica” of Cuilen
- studies the pharmacodynamic activity of Quinquina (Peruvian Bark – quinine)
- the first dynamized centesimal dilutions using tincture of Quinquina demonstrating by practice the ancient principle :

Similia similibus curantur

- repeats this procedure with mercury, Belladonna, digitalis
- does not succeed to continue his original medical practice in Germany
- moves in Paris and becomes in short time a famous personality

DYNAMIZED CENTESIMAL DILUTIONS

Basic Tincture of a specific active principle described in MATERIA MEDICA (usually a concentrated solution in EtOH)

1 – CH = 1 ml Tincture + 99 (or 100) ml distilled water

2 – CH = 1 ml (1 – CH) + 99 (or 100) ml distilled water

3 – CH = 1 ml (2 – CH) + 99 (or 100) ml distilled water

4 – CH = 1 ml (3 – CH) + 99 (or 100) ml distilled water

.

.

.

.

n – CH = 1 ml ((n-1)-CH) + 99 (or 100) ml distilled water

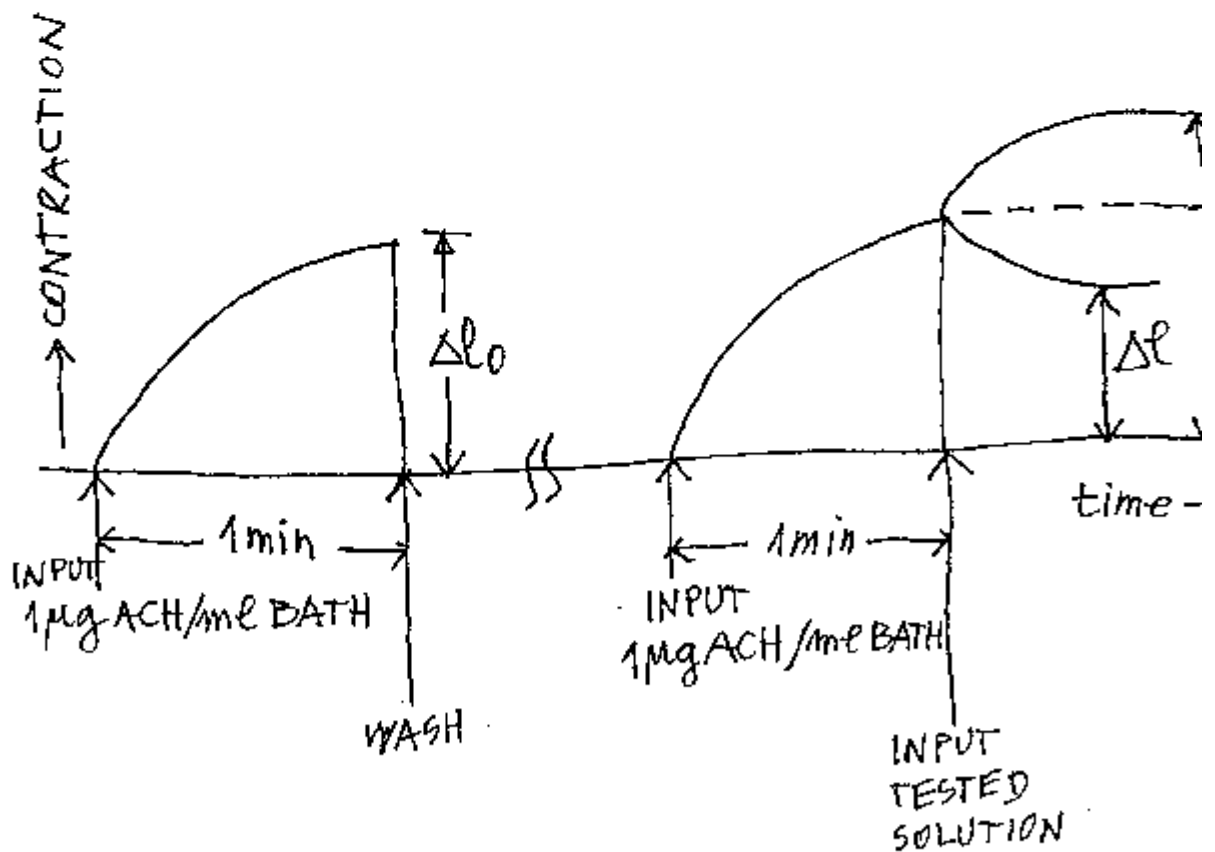
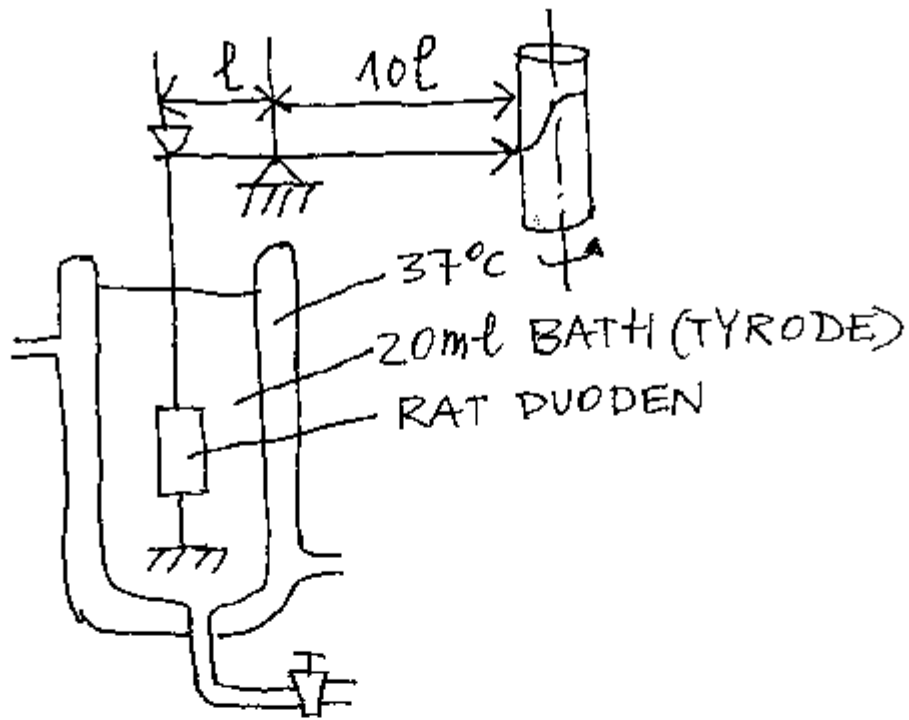
Each (n-CH) is DYNAMIZED before dilution.

Ex: active principle : Natrium Murriaticum (natural NaCl)
Centesimal dilutions by using EtOH (70%vol) as solvent.

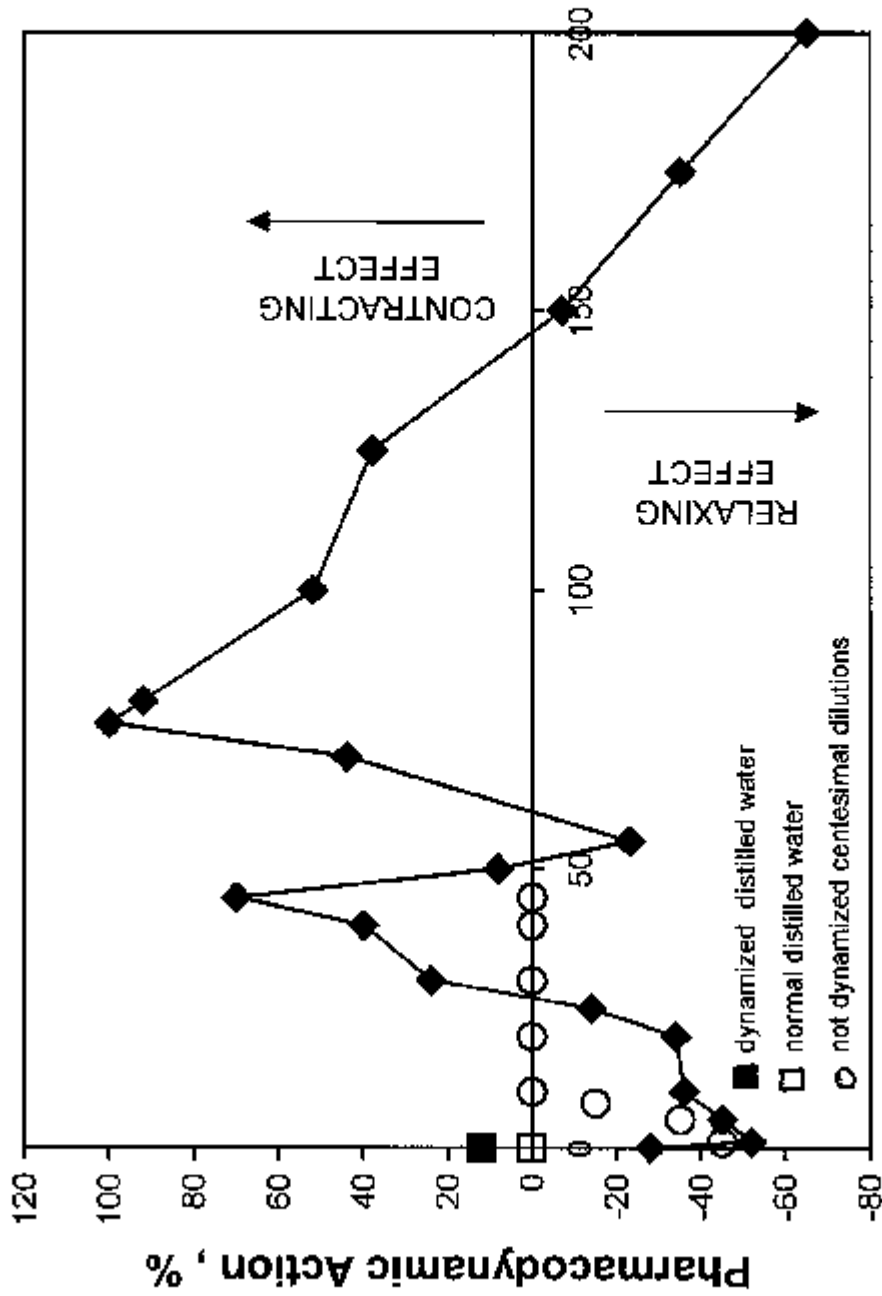
1986

High accuracy measurements on density and EtOH content:

Centesimal Dilutions	Density	EtOH content
Normal	Lower	lower
Dynamized	Higher	higher



$$\text{PHARMACODYNAMIC ACTIVITY [\%]} = (\Delta e - \Delta e_0) / \Delta e_0 \times 100$$



ORDER OF CENTESIMAL DILUTIONS , n - CH

Pharmacodynamic activity of dynamized centesimal solutions of

Belladonna as determined by the method of isolated organ

A. Cristea, G. Dragan, V. Darie : The 1st National Conference on Homeopathy ,
Sibiu , Romania, 12-13 October 1989